

Differential Privacy with Random Projections and Sign Random Projections

Ping Li, Xiaoyun Li

LinkedIn Ads

700 Bellevue Way NE, Bellevue, WA 98004, USA

{pinli, xiaoyli}@linkedin.com

Abstract

In this paper, we develop a series of differential privacy (DP) algorithms from a family of random projections (RP), for general applications in machine learning, data mining, and information retrieval. Among the presented algorithms, **iDP-SignRP** is remarkably effective under the setting of “individual differential privacy” (iDP), based on sign random projections (SignRP). Also, **DP-SignOPORP** considerably improves existing algorithms in the literature under the standard DP setting, using “one permutation + one random projection” (OPORP), where OPORP is a variant of the celebrated count-sketch method with fixed-length binning and normalization. Without taking signs, among the DP-RP family, **DP-OPORP** achieves the best performance.

The concept of iDP (individual differential privacy) is defined only on a particular dataset of interest. While iDP is not strictly DP, it might be useful in certain applications, such as releasing a dataset (including sharing embeddings across companies or countries). In our study, we find that **iDP-SignRP** is remarkably effective for search and machine learning applications, in that the utilities are exceptionally good even at a very small privacy parameter ϵ (e.g., $\epsilon < 0.5$).

Privacy can be protected at various stages of data life cycle. In this study, our methods can be applied as early as at data collection time. Instead of directly using the original p -dimensional vector u , we let $x_j = \sum_{i=1}^p u_i w_{ij}$, where $j = 1$ to k and w_{ij} is sampled from the Gaussian distribution. This is known as random projections (RP). In this paper, we assume the projection matrix $\{w_{ij}\}$ is also released to the public, as a stronger privacy setting. The previous algorithm named “DP-RP-G” can be improved quite considerably by setting the noise more carefully. The proposed new variant, named “DP-RP-G-OPT”, compares favorably with directly adding noise to the original data. DP-RP-G-OPT can be further improved by “DP-RP-G-OPT-B” by replacing the Gaussian projections with Rademacher projections due to the smaller sensitivity. Finally, via the fixed-length binning mechanism, “DP-OPORP” slightly outperforms DP-RP-G-OPT-B. Empirical evidence shows that these DP-RP algorithms require $\epsilon \approx 20$ to achieve a good utility.

Our key idea for improving DP-RP is to take only the signs, i.e., $sign(x_j) = sign(\sum_{i=1}^p u_i w_{ij})$, of the projected data. The intuition is that the signs often remain unchanged when the original data (u) exhibit small changes (according to the “neighbor” definition in DP). In other words, the aggregation and quantization operations themselves provide good privacy protections. We develop a technique called “**smooth flipping probability**” that incorporates this intuitive privacy benefit of SignRPs and improves the standard DP bit flipping strategy. Based on this technique, we propose **DP-SignOPORP** which satisfies strict DP and outperforms other DP variants based on SignRP (and RP), especially when ϵ is not very large (e.g., $\epsilon = 5 \sim 10$). Moreover, if an application scenario accepts individual DP, then we immediately obtain an algorithm named **iDP-SignRP** which achieves excellent utilities even at small ϵ (e.g., $\epsilon < 0.5$).

In practice, the main obstacle for deploying DP at the source of data is the severe degradation of performance because the amount of required noise is typically high. We hope our proposed series of DP (and iDP) algorithms, e.g., **DP-OPORP**, **DP-SignOPORP**, **iDP-SignRP**, will help promote the industrial applications of DP in search, retrieval, ranking, and AI in general.

Contents

1	Introduction	3
1.1	Random Projections (RP) and Very Sparse Random Projections (VSRP)	4
1.2	Sign Random Projections (SignRP)	4
1.3	Count-Sketch and OPORP: One Permutation + One Random Projection	5
1.4	DP Through RP and SignRP: Applications, Algorithms and Results	5
2	Preliminaries	7
2.1	Differential Privacy	7
2.2	Local Sensitivity and Smooth Sensitivity	9
2.3	Relaxation: Individual Differential Privacy (iDP)	10
3	DP-RP: Differentially Private Random Projections	11
3.1	Gaussian Noise Mechanism for DP-RP	11
3.2	The Optimal Gaussian Noise Mechanism for DP-RP	12
3.3	The Laplace Noise Mechanism for DP-RP	13
3.4	DP-RP-G-OPT-B: DP-RP with Rademacher Projections	14
3.5	DP-OPORP: A More Efficient Alternative	15
3.6	Comparison: Inner Product Estimation	17
4	DP-SignRP: Differentially Private Sign Random Projections	20
4.1	DP-SignRP-RR by Randomized Response	20
4.1.1	The flipping probability and calculation of N_+	21
4.1.2	Utility in angle estimation by DP-SignRP-RR	24
4.2	DP-SignRP-RR-Smooth Using Smooth Flipping Probability	26
4.3	DP-SignRP with Rademacher Projections	28
4.4	DP-SignOPORP with Smooth Flipping Probability	30
5	Experiments	32
5.1	Similarity Search	32
5.2	SVM Classification	34
5.3	Results for DP-SignOPORP	35
6	iDP-SignRP Under Individual Differential Privacy (iDP)	36
6.1	iDP-SignRP-G by Gaussian Noise Addition	36
6.2	iDP-SignRP-RR by Randomized Response	38
6.3	Empirical Results on iDP	39
7	Conclusion	40
A	Deferred Proofs	48
A.1	Proof of Lemma 3.6	48
A.2	Proof of Lemma 4.2	48

1 Introduction

With the rapid growth of capable electronic devices, personal data has been continuously collected by companies/organizations. Protecting data privacy has become an urgent need and a trending research topic in computer science, statistics, applied mathematics, etc. Among many notions of privacy, the “differential privacy” (DP) (Dwork et al., 2006) has gained tremendous attention in both the research community and industrial applications. The intuition of DP is straightforward:

We want to find a randomized data output procedure, such that a small change in the database can hardly be detected by an adversary based on the observation of the output.

Differential privacy provides a formal mathematical definition of privacy (see Section 2 for the details) that is powerful in the sense that it protects the sensitive data regardless of how the adversary utilizes the data subsequently. The strength of DP is usually characterized by two parameters, ϵ and δ . If $\delta = 0$, we say that the algorithm is “pure DP” (i.e., ϵ -DP); if $\delta > 0$, the algorithm is called “approximate DP” (i.e., (ϵ, δ) -DP). The typical technique of DP is to randomize/perturb the algorithm output by adding noise or probabilistic sampling. DP has been widely applied to numerous tasks such as clustering (Feldman et al., 2009; Gupta et al., 2010), regression and classification (Chaudhuri and Monteleoni, 2008; Zhang et al., 2012), DP-SGD (Abadi et al., 2016; Agarwal et al., 2018; Fang et al., 2023), principle component analysis (Ge et al., 2018), empirical risk minimization (Chaudhuri et al., 2011), matrix completion (Blum et al., 2005; Jain et al., 2018), graph distance estimation (Kasiviswanathan et al., 2013; Fan and Li, 2022; Fan et al., 2022). In industry, DP has been broadly deployed to collect user data for (e.g.,) frequency or mean estimation at, for example, Google (Erlingsson et al., 2014), Apple¹, and Microsoft (Ding et al., 2017).

The data to be protected may have various forms and come from various sources, for example: (i) the user “profile” vectors that contain sensitive attributes like personal information, click history, etc.; (ii) the embedding vectors learned from the user data, which may also contain rich information about the users and could be attacked by malicious adversaries to infer user attributes (Beigi et al., 2020; Zhang et al., 2021). In a machine learning model, there are several choices on when to deploy differential privacy (DP): (a) at the data collection/processing stage (Zhang et al., 2014; Yang et al., 2015; Berlioz et al., 2015; Cormode et al., 2018b); (b) during the model training stage (Abadi et al., 2016; Wei et al., 2020); and (c) on the model output (or summary data statistics) (Dwork and Lei, 2009). While each of them may find its need depending on the application scenarios, applying DP as early as at the data collection stage provides strong protection in the sense that the subsequent operations or outputs will become private by the post-processing property of differential privacy. Moreover, the data holder may need to release the data to third-parties. In this case, a private data publishing mechanism (at an early stage) becomes necessary.

In this work, we study differential privacy algorithms for protecting data vectors, based on the broad family of random projections (RP) and sign random projections (SignRP). Our algorithms can be applied to data publishing and processing for downstream machine learning tasks. In this paper, besides the standard DP, we also consider a relaxation of DP called “individual differential privacy” (iDP) (Soria-Comas et al., 2017), which was proposed with the aim of improving the utility of private algorithms. It turns out that, when it is applied to SignRP, iDP indeed provides a much better utility, a phenomenon which might be interesting to the DP researchers and practitioners and provides a plausible option for balancing the privacy and utility in practice.

¹<https://docs-assets.developer.apple.com/ml-research/papers/learning-with-privacy-at-scale.pdf>

1.1 Random Projections (RP) and Very Sparse Random Projections (VSRP)

In practice, compression and dimension reduction techniques can be crucial when dealing with massive (high-dimensional) data. The random projection (RP) method is an important fundamental algorithm. Denote $u \in \mathbb{R}^p$ as the data vector with p features. With some k (and typically $k \ll p$), we define the random projection of u as

$$X = \frac{1}{\sqrt{k}} W^T u, \quad W \in \mathbb{R}^{p \times k}. \quad (1)$$

The entries of the random matrix W typically follow the Gaussian distribution or Gaussian-like distribution such as uniform. It has been well-understood that, with a sufficient number of projections (k), the similarity between two vectors (using the same projection W) is preserved within a small multiplicative error with high probability. The dimensionality reduction and geometry preserving properties make RP widely useful in numerous applications, such as distance estimation, nearest neighbor search, clustering, classification, compressed sensing, etc. (Johnson and Lindenstrauss, 1984; Indyk and Motwani, 1998; Dasgupta, 2000; Bingham and Mannila, 2001; Achlioptas, 2003; Fern and Brodley, 2003; Vempala, 2005; Candès et al., 2006; Donoho, 2006; Li et al., 2006; Freund et al., 2007; Dasgupta and Freund, 2008; Dahl et al., 2013; Li and Li, 2019a; Rabanser et al., 2019; Tomita et al., 2020; Zhang and Li, 2020; Li and Li, 2023a).

Instead of using dense projections, it is also common to sample the entries of W from the following “very sparse” distribution, i.e., VSRP (Li et al., 2006):

$$\sqrt{s} \times \begin{cases} -1 & \text{with prob. } 1/(2s) \\ 0 & \text{with prob. } 1 - 1/s, \\ +1 & \text{with prob. } 1/(2s) \end{cases}, \quad (2)$$

which generalizes Achlioptas (2003) (for $s = 1$ and $s = 3$). Note that when $s = 1$, it is also called the “symmetric Bernoulli” distribution or the “Rademacher” distribution. In a recent study by Li and Li (2023a), the estimation accuracy of VSRP can be substantially improved via a normalization step.

1.2 Sign Random Projections (SignRP)

While RP is able to reduce the dimensionality to, e.g., hundreds, storing and transmitting the random projections might still be expensive for large datasets. To this regard, one can further compress the RPs by quantization/discretization, where we only use a few bits to represent the projected data, instead of using full-precision (32 or 64 bits). Quantized random projections (QRP) and the extensions (e.g., to non-linear kernels) have many applications in various fields, e.g., compressed sensing, approximate nearest neighbor search, similarity estimation, large-scale machine learning (Goemans and Williamson, 1995; Charikar, 2002; Datar et al., 2004; Boufounos and Baraniuk, 2008; Dong et al., 2008; Zymnis et al., 2010; Leng et al., 2014; Li et al., 2014; Knudson et al., 2016; Slawski and Li, 2018; Li, 2019; Li and Li, 2019b; Xu et al., 2021; Li and Li, 2021). In particular, in this paper, we will consider the differential privacy of the extreme case of sign (1-bit) random projection (SignRP), also known as the “SimHash” in the literature, where only the sign of the projected data is stored. Compared with storing the full-precision floats, SignRP provides substantial memory and communication saving which could be beneficial for large-scale databases.

From the sign random projections, one can estimate the angle/cosine between the data vectors. Consider two data vectors u and v with $\rho = \frac{u^T v}{\|u\| \|v\|}$ and $\theta = \cos^{-1}(\rho)$. Denote $x = \frac{1}{\sqrt{k}} W^T u$ and $y = \frac{1}{\sqrt{k}} W^T v$, with $x, y \in \mathbb{R}^k$. The standard result (Goemans and Williamson, 1995; Charikar, 2002) gives the collision probability for a single sign random projection as

$$Pr(\text{sign}(x_j) = \text{sign}(y_j)) = 1 - \frac{\theta}{\pi}, \quad \forall j = 1, \dots, k, \quad (3)$$

which leads to a straightforward estimator of the angle θ as

$$\hat{\theta} = \pi \left(1 - \frac{1}{k} \sum_{j=1}^k \mathbb{1}\{\text{sign}(x_j) = \text{sign}(y_j)\} \right). \quad (4)$$

As $\mathbb{1}\{\text{sign}(x_j) = \text{sign}(y_j)\}$ follows a Bernoulli distribution, the mean and variance of $\hat{\theta}$ can be precisely computed:

$$\mathbb{E}[\hat{\theta}] = \theta, \quad \text{Var}(\hat{\theta}) = \frac{\theta(\pi - \theta)}{k}. \quad (5)$$

In addition to the mentioned benefits of achieving highly compact representations of the original data, SignRP has also been widely used for approximate near neighbor (ANN) search (Friedman et al., 1975) by building hash tables from the SignRP bits (Indyk and Motwani, 1998; Charikar, 2002; Shrivastava and Li, 2014).

1.3 Count-Sketch and OPORP: One Permutation + One Random Projection

The celebrated count-sketch data structure (Charikar et al., 2004) can be viewed as a special type of very sparse projections. Count-sketch is highly efficient because, as an option, it only requires “one permutation + one random projection” (OPORP), as opposed to k projections. The recent work by Li and Li (2023a) improved the original count-sketch in two aspects: (i) Using a fixed-length binning scheme makes the algorithms more convenient and also reduces the variance by a factor of $\frac{p-k}{p-1}$. (ii) The projected data (i.e., vectors in k dimensions) should be normalized before they are used to estimate the original cosine. By doing so, the estimation variance can be substantially reduced, essentially from $(1 + \rho^2)/k$ (un-normalized) to $(1 - \rho^2)^2/k$ (normalized).

As the name OPORP suggests, the original data vector u is first permuted by a random permutation, and then it is divided into k bins. Within each bin, we apply a random projection of size p/k to obtain one projected value. Thus, we still obtain k projected values but the procedure is drastically more efficient than the standard random projections. The count-sketch data structure and variants have been widely used in applications. Recent examples include graph embedding (Wu et al., 2019), word & image embedding (Chen et al., 2017; Zhang et al., 2020; AlOmar et al., 2021; Singhal et al., 2021; Zhang et al., 2022), model & communication compression (Weinberger et al., 2009; Chen et al., 2015; Rothchild et al., 2020; Haddadpour et al., 2020; Li and Zhao, 2022) for linear models as well as deep neural nets, etc.

1.4 DP Through RP and SignRP: Applications, Algorithms and Results

In this paper, we propose to use random projection (RP) and sign random projection (SignRP) for data privatization. We name our methods “differentially private random projections” (DP-RP) and DP-SignRP. Additionally, we develop a series of algorithms for OPORP, named DP-OPORP and DP-SignOPORP. Finally, we will present iDP-SignRP using individual differential privacy (iDP).

The typical use cases of the proposed algorithms include:

- In on-device data collection, each user can apply our methods locally (with shared projection matrix/vectors) before sending the data to the server in the data collection process.
- At the central data silo, the data curator can first apply our methods to the data attributes (or embeddings) and then publish the output (randomized data) for data analysis or modeling.

By the geometry-preserving property of RP and SignRP, our approaches could be naturally and effectively applied to a variety of distance/similarity based downstream tasks like (approximate) nearest search, clustering, classification, and regression. Additionally, with DP-RP and DP-SignRP, the data compression (especially for high-dimensional datasets) is also able to consequently reduce the computational cost and the communication overhead when transmitting the data.

More specifically, for a data vector $u \in \mathbb{R}^p$, our goal is to make its RP and SignRP, namely $x = W^T u$ and $\text{sign}(X)$, differentially private. Then, for a database U consisting of n data vectors, applying this mechanism to all the points makes U differentially private against a change in one data record. In the literature, there are works on randomized algorithms that assume the randomness of the algorithm (e.g., the hash keys or projection matrices) are “internal” and also kept private (Blocki et al., 2012; Smith et al., 2020; Dickens et al., 2022). We assume the projection matrix W is known/public, which is stronger in privacy and enables broader applications of the released data. In addition, a “known projection matrix” is the typical case in the local DP model (Kairouz et al., 2014; Cormode et al., 2018a), since the projection matrix is created and shared among the users by the data aggregator.

In summary, in this paper we make the following contributions:

- In Section 3, for DP-RP, we first revisit/analyze the prior work (Kenthapadi et al., 2013) on the (ϵ, δ) -DP random projection based on Gaussian noise addition (called DP-RP-G). Then we propose an optimal Gaussian noise mechanism DP-RP-G-OPT, which improves the previous method. Then, we present DP-RP-G-OPT-B (which uses Rademacher projection and optimal noise) and DP-OPORP. We compare these variants of DP-RP with the strategy of adding (optimal) Gaussian noise to the raw data, in terms of the accuracy of inner product estimation.
- In Section 4, we propose two algorithms for privatizing the (1-bit) DP-SignRP. The first method, DP-SignRP-RR, is based on the standard “randomized response” (RR). Then, we propose an improved method named DP-SignRP-RR-smooth based on a proposed concept of “smooth flipping sensitivity”, thanks to the robustness brought by the “aggregate-and-sign” operation of SignRP. Finally, we extend the idea of smooth flipping probability to the OPORP variant, and show that DP-SignOPORP is more advantageous in terms of differential privacy.
- In Section 5, we conduct retrieval and classification experiments on benchmark datasets. Specifically, for DP-RP, the proposed optimal DP-RP-G-OPT method substantially improves DP-RP-G, which is the previous DP-RP method in the literature. DP-OPORP performs similarly to DP-RP-G-OPT-B. For the 1-bit variants, our proposed DP-SignOPORP outperforms DP-RP variants and DP-OPORP especially when ϵ is not large (e.g., $\epsilon = 5 \sim 10$).
- In Section 6, we further design iDP-SignRP algorithms under the setting of individual differential privacy (iDP), which is a relaxed definition of the standard DP (Soria-Comas et al., 2017). Experiments demonstrate that iDP-SignRP is able to achieve excellent utilities (precision, recall, classification accuracy) even when ϵ is small (e.g., $\epsilon < 0.5$). We anticipate that iDP-SignRP will be useful (e.g.,) as a data-publishing mechanism, among other applications.

2 Preliminaries

Throughout the paper, $\|\cdot\|_1$ and $\|\cdot\|_2$ are the l_1 and l_2 norms, respectively. For convenience, $\|\cdot\|$ will denote the l_2 norm if there is no risk of confusion. Let $u \in \mathbb{R}^p$ be a data vector of p dimensions. We assume $\|u\| > 0$, i.e., there is no all-zero data sample.

2.1 Differential Privacy

Differential privacy (DP) has been one of the standard tools in the literature to protect against (e.g.,) attribute inference attacks. The formal definition of DP is as follows.

Definition 2.1 (Differential Privacy (Dwork et al., 2006)). *For a randomized algorithm $\mathcal{M} : \mathcal{U} \mapsto \text{Range}(\mathcal{M})$, if for any two adjacent datasets u and u' , it holds that*

$$\Pr[\mathcal{M}(u) \in O] \leq e^\epsilon \Pr[\mathcal{M}(u') \in O] + \delta \quad (6)$$

for $\forall O \subset \text{Range}(\mathcal{M})$ and some $\epsilon, \delta \geq 0$, then algorithm \mathcal{M} is called (ϵ, δ) -differentially private. If $\delta = 0$, \mathcal{M} is called ϵ -differentially private.

Consider the classic noise addition approaches in DP. Given some definition of “neighboring”, one important quantity is the “sensitivity” described below.

Definition 2.2 (Sensitivity). *Let $Nb(u)$ denote the neighbor set of u , and $\mathcal{N}(\mathcal{U}) = \{(u, u') : u' \in Nb(u), u, u' \in \mathcal{U}\}$ be the collection of all possible neighboring data pairs. The l_1 -sensitivity and l_2 -sensitivity of a function $f : \mathcal{U} \mapsto \mathbb{R}^k$ are defined respectively as*

$$\Delta_1 = \max_{(u, u') \in \mathcal{N}(\mathcal{U})} \|f(u) - f(u')\|_1, \quad \Delta_2 = \max_{(u, u') \in \mathcal{N}(\mathcal{U})} \|f(u) - f(u')\|_2.$$

In this work, our goal is to protect the data itself independent of subsequent tasks or operations. We follow the natural and standard definition in the DP literature of “neighboring” for data vectors, that two vectors are adjacent if they differ in one element (e.g., Dwork et al. (2006); Kenthapadi et al. (2013); Xu et al. (2013); Dwork and Roth (2014); Smith et al. (2020); Stausholm (2021); Dickens et al. (2022); Zhao et al. (2022); Li and Li (2023b)).

Definition 2.3 (β -adjacency). *Let $u \in [-1, 1]^p$ be a data vector. A vector $u' \in [-1, 1]^p$ is said to be β -adjacent to u if u' and u differ in one dimension i , and $|u_i - u'_i| \leq \beta$.*

Data vectors u and u' satisfying Definition 2.3 are called β -adjacent or β -neighboring. Several remarks follow:

- Compared with l_1 difference: $\|u - u'\|_1 \leq \beta$, Definition 2.3 (i.e., u' and u differ in one dimension i with $|u_i - u'_i| \leq \beta$) considers the worst case of the l_1 difference in sensitivity analysis.
- In the literature (e.g., Kenthapadi et al. (2013) for RP), $\beta = 1$ is typically used. We allow a more general β to accommodate the need from practical applications.
- Assuming $u \in [-1, 1]^p$ is merely for convenience, as one can easily extend the results to $u \in [-C, C]^p$ for an arbitrary $C > 0$. Note that, coincidentally, the “max normalization” is a common data pre-processing strategy, where each feature dimension is normalized to $[-1, 1]$.

We make a more detailed explanation of the first point above. Since the neighboring data vector u' and the raw data u only differ in one attribute by at most β , by Definition 2.2, it is easy to see that for RP the sensitivities are precisely $\frac{1}{\sqrt{k}}$ times the largest row norm of W :

$$\Delta_1 = \frac{1}{\sqrt{k}}\beta \max_{(u,u') \in \mathcal{N}(\mathcal{U})} \|W^T u - W^T u'\|_1 = \frac{1}{\sqrt{k}}\beta \max_{i=1,\dots,p} \|W_{[i,:]\|_1, \quad (7)$$

$$\Delta_2 = \frac{1}{\sqrt{k}}\beta \max_{(u,u') \in \mathcal{N}(\mathcal{U})} \|W^T u - W^T u'\|_2 = \frac{1}{\sqrt{k}}\beta \max_{i=1,\dots,p} \|W_{[i,:]\|_2. \quad (8)$$

where $W_{[i,:]$ is the i -th row of W . It is a known fact that Definition 2.3 for neighboring is the worst case for the alternative neighboring definition using the l_1 difference: “ u and u' are neighboring if $\|u - u'\|_1 = \sum_{i=1}^p |u_i - u'_i| \leq \beta$.” Particularly, in our work, we have $f(u) = \frac{1}{\sqrt{k}}W^T u$, and thus

$$\begin{aligned} \frac{1}{\sqrt{k}} \max_{\|u-u'\|_1 \leq \beta} \|W^T u - W^T u'\|_1 &= \frac{1}{\sqrt{k}} \max_{\|u-u'\|_1 \leq \beta} \left\| \sum_{i=1}^p (u_i - u'_i) W_{[i,:]\right\|_1 \\ &\leq \frac{1}{\sqrt{k}} \max_{\|u-u'\|_1 \leq \beta} \sum_{i=1}^p |u_i - u'_i| \|W_{[i,:]\|_1 \\ &= \frac{1}{\sqrt{k}}\beta \max_{i=1,\dots,p} \|W_{[i,:]\|_1 = \Delta_1. \end{aligned}$$

Note that the last line equals (7) corresponding to the sensitivity based on Definition 2.3. Since the neighboring condition in Definition 2.3 also satisfies $\|u - u'\|_1 \leq \beta$, we know that the equality can be exactly attained. Similarly, for the l_2 sensitivity, we have

$$\begin{aligned} \frac{1}{\sqrt{k}} \max_{\|u-u'\|_1 \leq \beta} \|W^T u - W^T u'\|_2 &= \frac{1}{\sqrt{k}} \max_{\|u-u'\|_1 \leq \beta} \left\| \sum_{i=1}^p (u_i - u'_i) W_{[i,:]\right\|_2 \\ &= \frac{1}{\sqrt{k}}\beta \max_{i=1,\dots,p} \|W_{[i,:]\|_2 = \Delta_2. \end{aligned}$$

Therefore, for the sensitivity analysis, the “ β -adjacency” in Definition 2.3 in fact covers the definition of neighboring based on the l_1 difference.

Once the sensitivities can be identified/computed, the following two standard noise addition mechanisms can be applied to make an algorithm differentially private.

Theorem 2.1 (Laplace mechanism (Dwork et al., 2006)). *Given any function $f : \mathcal{U} \mapsto \mathbb{R}^k$ and $\epsilon > 0$, the randomized algorithm $\mathcal{M}(u) = f(u) + (Z_1, \dots, Z_k)$ is ϵ -DP, where Z_1, \dots, Z_k follow iid Laplace(Δ_1/ϵ). The centered Laplace distribution with scale λ has density function $g(x) = \frac{1}{2\lambda} e^{-\frac{|x|}{\lambda}}$.*

Theorem 2.2 (Gaussian mechanism (Dwork and Roth, 2014)). *Given any function $f : \mathcal{U} \mapsto \mathbb{R}^k$, $0 < \epsilon < 1$, $0 < \delta < 1$, the randomized algorithm $\mathcal{M}(u) = f(u) + (Z_1, \dots, Z_k)$ is (ϵ, δ) -DP, where Z_1, \dots, Z_k follow iid $N(0, \sigma^2)$ with $\sigma = \Delta_2 \frac{\sqrt{2 \log(1.25/\delta)}}{\epsilon}$.*

We remark that Theorem 2.2 requires $\epsilon < 1$. The behavior of the Gaussian noise for general ϵ will be discussed shortly in Section 3. Furthermore, one of the nice facts about DP is that, multiple DP algorithms can be composed together, where the final output is still DP.

Theorem 2.3 (Composition Theorem (Dwork and Roth, 2014)). *Let $\mathcal{M}_j : \mathcal{U} \rightarrow \mathbb{R}$ be an (ϵ_j, δ_j) -DP algorithm for $j = 1, \dots, k$. Then $\mathcal{M}(u) = (\mathcal{M}_1(u), \dots, \mathcal{M}_k(u))$ is $(\sum_{j=1}^k \epsilon_j, \sum_{j=1}^k \delta_j)$ -DP.*

2.2 Local Sensitivity and Smooth Sensitivity

The sensitivity in Definition 2.2 is a “global” worst-case bound over all possible neighboring data (u, u') in the data domain, which in many cases leads to overly large noise added to the algorithm output. Intuitively, for each specific data u , to make $\mathcal{M}(u)$ and $\mathcal{M}(u')$ indistinguishable in the sense of DP, we may not always need the worst-case noise. This is grasped by the concept of “local sensitivity” as defined below.

Definition 2.4 (Local sensitivity (Nissim et al., 2007)). *For $u \in \mathcal{U}$ and a function $f : \mathcal{U} \mapsto \mathbb{R}^k$, the local sensitivities of f at u are*

$$LS_1(u) = \max_{u' \in Nb(u)} \|f(u) - f(u')\|_1, \quad LS_2(u) = \max_{u' \in Nb(u)} \|f(u) - f(u')\|_2.$$

Instead of bounding the worst-case change in the output, the local sensitivity at u just focuses on the neighborhood of each specific u . By the definitions, it is clear that $LS_1(u) \leq \Delta_1$ and $LS_2(u) \leq \Delta_2$ for all $u \in \mathcal{U}$, i.e., the global sensitivity is an upper bound of local sensitivity. That said, the noise level calibrated to the local sensitivity is always smaller than the noise magnitude calculated by the global sensitivity, which implies (substantially) better utility.

One however cannot simply add noise according to the instance-specific local sensitivity to achieve DP, for several reasons. (A) Only ensuring “local” indistinguishability at each specific data instance does not satisfy the rigorous DP condition (Definition 2.1), which requires the indistinguishability between all possible adjacent data pairs. (B) The noise level itself, when computed by the local sensitivity, is a function of u , which may reveal the information of the database. Intuitively, the issue of local sensitivity is that, although u has small local sensitivity, its neighbor u' may have very large local sensitivity. If the injected noise is determined according to the local sensitivity, then the very different noise scale may be detected by an adversary to distinguish u from u' , violating the goal of DP. A simple example is provided in Nissim et al. (2007) for reporting the median. In that same paper, the authors proposed “smooth sensitivity” which leverages local sensitivity in the noise calibration, at the same time also satisfies the DP definition. The intuition is that, whatever “local” notion of sensitivity at u we employ must account for the more sensitive data which are nearby, but at a discounted factor depending on how far they are from u .

Definition 2.5 (Smooth sensitivity (Nissim et al., 2007)). *For $u, u' \in \mathcal{U}$, denote $d(u, u')$ as the minimal number of “neighboring operations” needed to derive u' from u ². The ϵ -smooth sensitivity of $f : \mathcal{U} \mapsto \mathbb{R}^k$ at u is defined as*

$$SS(u) = \max_{u' \in \mathcal{U}} e^{-\epsilon d(u, u')} LS(u'),$$

where $LS(u')$ is the local sensitivity (in proper metric) of f at u' in Definition 2.4.

The smooth sensitivity $SS(u)$ is an ϵ -smooth upper bound of the local sensitivity $LS(u)$ satisfying two conditions: (i) $SS(u) \geq LS(u)$, $\forall u \in \mathcal{U}$; (ii) $SS(u) \leq e^\epsilon SS(u')$, $\forall u, u' \in \mathcal{U}$ with $d(u, u') = 1$. Moreover, $SS(u)$ is the smallest upper bound $\forall u$ among all such ϵ -smooth upper bounds³. Nissim et al. (2007) also proposed several noise addition mechanisms tailored to the (instance-specific) smooth sensitivity, with rigorous DP guarantees. In particular, the smooth sensitivity usually works very well for robust statistics/estimators (e.g., the median, the interquartile range), in which the local sensitivity in the neighborhood of most data does not change much.

²For example, if u and u' are two databases that differ in t sample records, then $d(u, u') = t$.

³The global sensitivity (Definition 2.2) is also an ϵ -smooth upper bound of the local sensitivity.

For DP-RP studied in our paper, it is easy to check that both the local sensitivity and smooth sensitivity, at any $u \in [-1, 1]^p$, are the same as the global sensitivity by (7) and (8). Thus, for DP-RP, these two concepts may not help much. Fortunately, for DP-SignRP, the “aggregate-and-sign” operation brings robustness against small data changes. Therefore, we can leverage the idea of local or smooth sensitivity to develop novel and better DP algorithms than the standard bit/sign flipping approach (Section 4.2 and Section 6).

2.3 Relaxation: Individual Differential Privacy (iDP)

Besides the smooth sensitivity framework, many extensions or relaxations of DP have also been proposed to improve the utility of DP mechanisms. Examples include concentrated differential privacy (Dwork and Rothblum, 2016), Rényi differential privacy (Mironov, 2017), and Gaussian differential privacy (Dong et al., 2022). These alternatives provide less strict requirement on the “indistinguishability” (6) for privacy and better composition properties than those of the standard “worst-case” DP, thus reducing the noise needed (Jayaraman and Evans, 2019). Another possible direction to elevate the empirical performance of DP is to relax the DP definition by constraining the scope of neighboring datasets depending on the specific use case of DP (Soria-Comas et al., 2017; Desfontaines and Pejó, 2020). In this paper, we also consider the concept called “individual differential privacy” (iDP), also known as “data-centric DP”, as follows.

Definition 2.6 (Individual DP (Soria-Comas et al., 2017)). *Given a dataset u , an algorithm \mathcal{M} satisfies (ϵ, δ) -iDP for u if for any dataset u' that is adjacent to u , it holds that*

$$\begin{aligned} Pr[\mathcal{M}(u) \in O] &\leq e^\epsilon Pr[\mathcal{M}(u') \in O] + \delta, \\ Pr[\mathcal{M}(u') \in O] &\leq e^\epsilon Pr[\mathcal{M}(u) \in O] + \delta. \end{aligned}$$

We should emphasize that, individual DP does not satisfy the rigorous DP definition, as iDP only focuses on the “point-wise” guarantee of privacy. It protects the neighborhood of a specific dataset of interest, instead of fulfilling DP requirements for all possible adjacent databases. While deviating from the standard DP definition, we discuss it in our work because iDP might be sufficient for some applications, and the utility gain of iDP can be substantial.

The intuition of iDP is that, while the standard DP (Definition 2.1) requires indistinguishability between any pair of neighboring databases, in some practical scenarios, the data custodian only holds one “ground truth” data vector u that needs to be protected. Limiting the scope of the neighborhood could be reasonable in certain practical scenarios. For example, for the centralized data server to (non-interactively) publish the user data matrix or user embedding vectors to the public, we essentially care about preserving the privacy of the true user data at hand, as no information other than the perturbed database would be released. In this paper, while we will mainly focus on the standard DP definition, we also find that using iDP for sign-based RP methods provides good utilities. Therefore, we will also discuss iDP-based variants in Section 6, as it may provide another direction/option for balancing the trade-off between privacy and utility in practice, based on specific applications.

3 DP-RP: Differentially Private Random Projections

In this section, we study the differentially private random projections (DP-RP). We first revisit the noise addition mechanisms reported in [Kenthapadi et al. \(2013\)](#) for Gaussian random projections, an algorithm which we name “DP-RP-G”. Then we apply the optimal Gaussian mechanism ([Balle and Wang, 2018](#)) to DP-RP to obtain an improved algorithm named “DP-RP-G-OPT”. In [Section 5](#), our experiments confirm that DP-RP-G-OPT considerably improves DP-RP-G. Moreover, by replacing the Gaussian projection matrix with the Rademacher projection matrix, we obtain a further improved version named “DP-RP-G-OPT-B”. Furthermore, one can obtain another variant called “DP-OPORP” by replacing the dense Rademacher projections with OPORP, which is a variant of count-sketch and is computationally much more efficient than dense projections.

We also analytically compare those variants of DP-RP with the basic DP strategy of directly adding Gaussian noise to each dimension of the original data vectors. Our analysis explains the improvements by using DP-RP in high-dimensional data.

3.1 Gaussian Noise Mechanism for DP-RP

Algorithm 1: DP-RP-G and DP-RP-G-OPT

- 1 **Input:** Data $u \in [-1, 1]^p$, privacy parameters $\epsilon > 0$, $\delta \in (0, 1)$, number of projections k
 - 2 **Output:** (ϵ, δ) -differentially private random projections $\tilde{x} \in \mathbb{R}^k$
 - 3 Apply RP $x = \frac{1}{\sqrt{k}}W^T u$, where $W \in \mathbb{R}^{p \times k}$ has iid entries sampled from $N(0, 1)$
 - 4 Compute the sensitivity Δ_2 by [\(8\)](#)
 - 5 Generate the random noise vector $G \in \mathbb{R}^k$ whose entries are iid samples from $N(0, \sigma^2)$ where σ is obtained by [Theorem 3.1](#) (DP-RP-G) or [Theorem 3.5](#) (DP-RP-G-OPT)
 - 6 Return $\tilde{x} = x + G$
-

The general Gaussian noise mechanism for DP-RP is detailed in [Algorithm 1](#). We present the algorithms for a single data point u , and the procedure is applied to every data vector in the database (with same W but independent noise). Given the projection matrix $W \in \mathbb{R}^{d \times k}$, we first compute the l_2 -sensitivity Δ_2 of the RPs according to [\(8\)](#). Then we generate the random Gaussian noise vector following iid $N(0, \sigma^2)$ where σ is derived by [Theorem 3.1](#) below, and output the projected vector plus the noise. The following Gaussian mechanism for random projections is known in the literature. We call it the “DP-RP-G” method.

Theorem 3.1 (DP-RP-G ([Kenthapadi et al., 2013](#))). *Let Δ_2 be defined in [\(8\)](#). For any $\epsilon > 0$ and $0 < \delta < \frac{1}{2}$, DP-RP-G in [Algorithm 1](#) is (ϵ, δ) -DP if $\sigma \geq \Delta_2 \frac{\sqrt{2(\log(1/\delta)+\epsilon)}}{\epsilon}$.*

According to [Theorem 3.1](#), one will choose σ based on the observed Δ_2 which is calculated according to [\(8\)](#) for a given realization of the projection matrix W . For the convenience of theoretical analysis, it is often desirable to derive the criterion for choosing σ directly in terms of the input parameters ϵ , δ , p , and k . We call the corresponding algorithm to be “Analytic DP-RP-G”. This is achieved by bounding Δ_2 in high probability.

Lemma 3.2 ([Laurent and Massart \(2000\)](#)). *Let Y_1, \dots, Y_n be iid standard Gaussian random variables, and denote $Z_i = \sum_{i=1}^n Y_i^2$. Then for any $t > 0$,*

$$Pr(Z \geq n + 2\sqrt{nt} + 2t) \leq \exp(-t).$$

Lemma 3.3 (Bounding Δ_2). Let $W \in \mathbb{R}^{p \times k}$ be a random matrix with iid $N(0, 1)$ entries, and Δ_2 be defined in (8). Then for any $0 < \delta < 1$,

$$\Pr \left(\Delta_2 \geq \beta \sqrt{1 + 2\sqrt{\log(p/\delta)/k} + 2\log(p/\delta)/k} \right) \leq \delta.$$

Proof. Let e_i be the unit base vector with the i -th dimension being 1 and all other dimensions being zero. For each $i = 1, \dots, p$, $W^T e_i$ follows iid chi-square distribution with k degree of freedom. Applying Lemma 3.2 we have that for any $\delta' > 0$,

$$\Pr \left(\|W^T e_i\|^2 \geq k + 2\sqrt{k \log(1/\delta')} + 2\log(1/\delta') \right) \leq \delta', \quad \forall i = 1, \dots, p.$$

Applying union bound gives

$$\Pr \left(\frac{1}{k} \beta^2 \max_{i=1, \dots, p} \|W^T e_i\|^2 \geq \beta^2 \left(1 + 2\sqrt{\log(1/\delta')/k} + 2\log(1/\delta')/k \right) \right) \leq p\delta'.$$

Setting $\delta = p\delta'$ and taking the square root on both sides completes the proof. \square

With the high probability bound on the l_2 -sensitivity Δ_2 , we have the following result.

Theorem 3.4 (Analytic DP-RP-G). For any $\epsilon > 0$ and $0 < \delta < \frac{1}{2}$, Algorithm 1 achieves (ϵ, δ) -DP when $\sigma \geq \frac{\beta \sqrt{1 + 2\sqrt{\log(2p/\delta)/k} + 2\log(2p/\delta)/k} \sqrt{2(\log(2/\delta) + \epsilon)}}{\epsilon}$.

Proof. By Lemma 3.3, with probability $\delta/2$, Δ_2 is bounded by $\beta \sqrt{1 + 2\sqrt{\log(2p/\delta)/k} + 2\log(2p/\delta)/k}$.

In this event, by Theorem 3.1, Algorithm 1 is $(\epsilon, \delta/2)$ -DP when $\sigma \geq \Delta_2 \frac{\sqrt{2(\log(2/\delta) + \epsilon)}}{\epsilon}$. Therefore, the approach is (ϵ, δ) -DP. \square

We remark that, since this analytic version is built upon a high probability bound on the sensitivity, in most cases, the noise variance in Theorem 3.4 will be slightly larger than the one computed by the realized/exact sensitivity in Theorem 3.1.

3.2 The Optimal Gaussian Noise Mechanism for DP-RP

In Theorem 3.1 (as well as the classical Gaussian mechanism, e.g., Dwork and Roth (2014)), the analysis on the noise level is based on upper bounding the tail of Gaussian distribution⁴. While the noise level in Theorem 3.1 is rate optimal (see Remark 3.1), it can be improved by computing the exact tail probabilities instead of the upper bounds. Balle and Wang (2018, Theorem 8) proposed the optimal Gaussian mechanism based on this idea, using which allows us to improve Theorem 3.1 and obtain the optimal DP-RP-Gaussian-Noise (DP-RP-G-OPT) method as follows.

Theorem 3.5 (DP-RP-G-OPT). Suppose Δ_2 is defined as (8). For any $\epsilon > 0$ and $0 < \delta < 1$, DP-RP-G-OPT in Algorithm 1 achieves (ϵ, δ) -DP if $\sigma \geq \sigma^*$ where σ^* is the solution to the equation

$$\Phi \left(\frac{\Delta_2}{2\sigma} - \frac{\epsilon\sigma}{\Delta_2} \right) - e^\epsilon \Phi \left(-\frac{\Delta_2}{2\sigma} - \frac{\epsilon\sigma}{\Delta_2} \right) = \delta, \quad (9)$$

where $\Phi(\cdot)$ is the cumulative distribution function (cdf) of the standard normal distribution.

⁴More specifically, the analysis of the classic Gaussian mechanism is based on bounding the probability of $X = \log \frac{p_{\mathcal{M}(u)}(y)}{p_{\mathcal{M}(u')}(y)} \geq \epsilon$, where u and u' are neighboring databases and y is an output. X , called the privacy loss random variable, is shown to follow a Gaussian distribution (Dwork and Rothblum, 2016) when the injected noise is Gaussian. The tail probability of X is then bounded by standard concentration inequalities.

Remark 3.1. For both Theorem 3.5 and Theorem 3.1, the Gaussian noise level is $\sigma = \mathcal{O}(\frac{\Delta_2}{\epsilon}) = \mathcal{O}(\frac{1}{\epsilon})$ when ϵ is small (i.e., $\epsilon \rightarrow 0$), and $\sigma = \mathcal{O}(\frac{1}{\sqrt{\epsilon}})$ when ϵ is large (i.e., $\epsilon \rightarrow \infty$). This is rate optimal as Gaussian mechanism must incur a noise $\sigma = \Omega(\frac{\Delta_2}{\sqrt{\epsilon}})$ when $\epsilon \rightarrow \infty$ (Balle and Wang, 2018). Theorem 3.5 reduces the variance of Theorem 3.1 by analyzing the tail probability exactly.

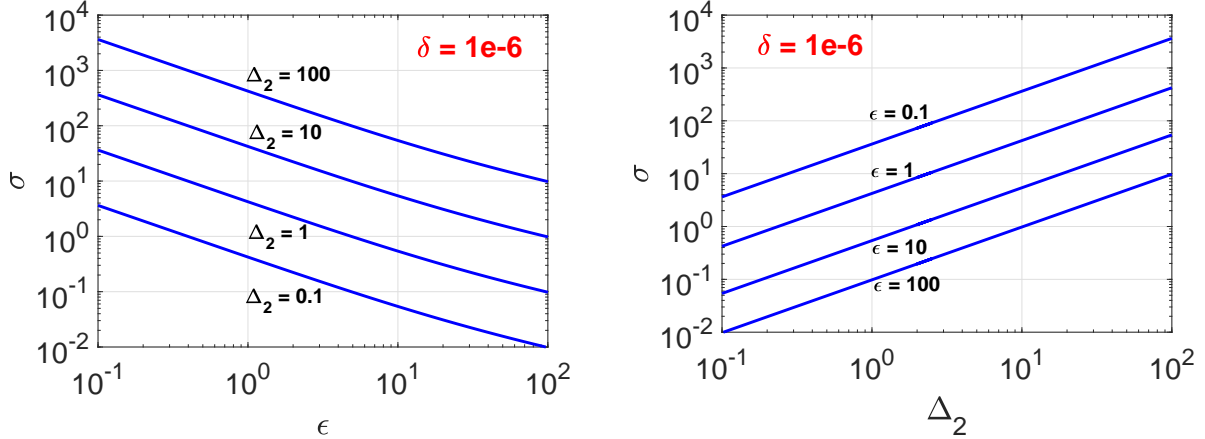


Figure 1: Left panel: the optimal Gaussian noise σ versus ϵ for a series of Δ_2 values, by solving the nonlinear equation (9) in Theorem 3.5, for $\delta = 10^{-6}$. Right panel: the optimal Gaussian noise σ versus Δ_2 for a series of ϵ values.

3.3 The Laplace Noise Mechanism for DP-RP

Algorithm 2: DP-RP-L

- 1 **Input:** Data $u \in [-1, 1]^p$, privacy parameters $\epsilon > 0$, number of projections k
 - 2 **Output:** ϵ -differentially private random projections $\tilde{x} \in \mathbb{R}^k$
 - 3 Apply RP $x = \frac{1}{\sqrt{k}} W^T u$, where $W \in \mathbb{R}^{p \times k}$ is a random $N(0, 1)$ matrix
 - 4 Compute sensitivity Δ_1 by (7)
 - 5 Generate iid random noise vector $L \in \mathbb{R}^k$ following $Laplace(\frac{\Delta_1}{\epsilon})$
 - 6 Return $\tilde{x} = x + L$
-

By Theorem 2.1, one may add $Laplace(\lambda)$ noise to the projected data with $\lambda = \Delta_1/\epsilon$ to achieve ϵ -DP. For completeness, we detail the approach in Algorithm 2, which is the same as Algorithm 1 except for the noise added. Δ_1 is the l_1 -sensitivity for a given W given in (7): $\Delta_1 = \frac{1}{\sqrt{k}} \beta \max_{i=1, \dots, p} \|W_{[i, :]}\|_1$. Each term in the maximum operator is a sum of k iid standard half-normal random variables ($Y = |X|$ where X is standard normal). The readers might be interested in a comparison between the noise level of the two noise addition mechanisms, i.e., DP-RP-G and DP-RP-L. To observe the dependence of the noise level λ on ϵ , k and p , we derive a tail bound on the l_1 -sensitivity. We first establish the following lemma.

Lemma 3.6 (Half-normal tail bound). *Let X_1, \dots, X_n be iid $N(0, 1)$ random variables and let $Y_i = |X_i|, \forall i$. Denote $Z = \sum_{i=1}^n Y_i$. Then for any $t > 0$, it holds that*

$$Pr(Z \geq \sqrt{2n^2 \log 2 + 2nt}) \leq \exp(-t).$$

Using Lemma 3.6, we obtain a high probability bound on the l_1 -sensitivity as follows. The proof is omitted since it is similar to the proof of Lemma 3.3.

Lemma 3.7 (Bounding Δ_1). *Let $W \in \mathbb{R}^{p \times k}$ be a random matrix with iid $N(0, 1)$ entries, and Δ_1 be defined in (7). Then for any $0 < \delta < 1$,*

$$\Pr \left(\Delta_1 \geq \beta \sqrt{2k \log 2 + 2 \log(p/\delta)} \right) \leq \delta.$$

It is important to point out that, unlike in the Gaussian mechanism, simply inserting the upper bound in Lemma 3.7 to replace the (exact) Δ_1 in the noise level of $Laplace(\Delta_1/\epsilon)$ in Algorithm 2 does not provide pure ϵ -DP. In other words, we must compute the actual Δ_1 by (7) for a realization of the projection matrix W . This is because, using the high probability bound of Δ_1 would introduce a failure probability (i.e., when the actual Δ_1 is larger than the bound) which violates ϵ -DP.

Comparison with DP-RP-G-OPT. Lemma 3.7 provides an estimate of the noise level required by the Laplace mechanism. We can roughly compare DP-RP-L with DP-RP-OPT in terms of the noise variances, which equal σ^2 for Gaussian and $2\lambda^2$ for Laplace, respectively. Lemma 3.7 shows that in most cases, the Laplace noise requires $\lambda = \mathcal{O}(\frac{\sqrt{k}}{\epsilon})$. Recall that in DP-RP-G and DP-RP-G-OPT, the Gaussian noise level $\sigma = \mathcal{O}(\frac{1}{\epsilon})$ when $\epsilon \rightarrow 0$ and $\sigma = \mathcal{O}(\frac{1}{\sqrt{\epsilon}})$ when $\epsilon \rightarrow \infty$. Thus, the Gaussian noise would be smaller with relatively small ϵ , and the Laplace noise would be smaller only when $\epsilon = \Omega(k)$, which is usually too large to be useful since in practice k is usually hundreds to thousands. As a result, we would expect DP-RP-G methods to perform better than DP-RP-L in common scenarios. Therefore, in the remaining parts of the paper, we will mainly focus on the Gaussian mechanism for noise addition.

3.4 DP-RP-G-OPT-B: DP-RP with Rademacher Projections

We have considered the Gaussian random projections. We can also adopt other types of projection matrices which might even work better for DP. The following distributions of w_{ij} are popular:

- The uniform distribution, $\sqrt{3} \times \text{unif}[-1, 1]$. The $\sqrt{3}$ factor is placed here to have $\mathbb{E}(w_{ij}^2) = 1$ by following the convention in the practice of random projections.
- The “very sparse” distribution, as used in Li et al. (2006):

$$w_{ij} = \sqrt{s} \times \begin{cases} -1 & \text{with prob. } 1/(2s) \\ 0 & \text{with prob. } 1 - 1/s, \\ +1 & \text{with prob. } 1/(2s) \end{cases} \quad (10)$$

which generalizes Achlioptas (2003) (for $s = 1$ and $s = 3$). Note that when $s = 1$, it is also called the “symmetric Bernoulli” distribution or the “Rademacher” distribution.

From Theorem 3.1 and Theorem 3.5, it is clear that the noise magnitude of Gaussian noise in DP-RP directly depends on the l_2 -sensitivity Δ_2 , which, according to (8), equals the largest row norm of the projection matrix W . Among the above-mentioned distributions, the dense Rademacher projection ($s = 1$ in (10)) has $\Delta_2 = \frac{1}{\sqrt{k}}\beta \times \sqrt{k} = \beta$ which is independent of p . This could be much smaller than the dense Gaussian projection (i.e., DP-RP-G-OPT) as can be seen from the bound in Lemma 3.3).

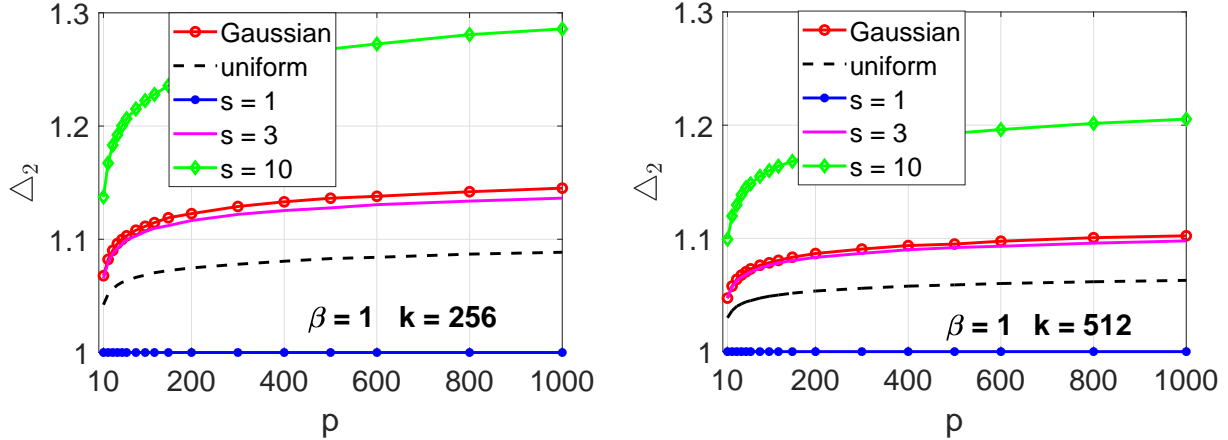


Figure 2: The l_2 -sensitivity Δ_2 (8) for different types of random projection matrices against the data dimensionality p , at $k = 256$ and $k = 512$, respectively. $\beta = 1$.

In Figure 2, we numerically simulate the Δ_2 of different projection matrices, which shows that the Rademacher projection produces the smallest sensitivity. This, when plugged into the optimal Gaussian mechanism (Theorem 3.5), leads to smaller Gaussian noise variance needed. For clarity, we summarize the DP-RP based on Rademacher projections in Algorithm 3. We name it “DP-RP-G-OPT-B”, where “G” stands for the **G**aussian noise mechanism and “B” stands for “symmetric Bernoulli” projections.

Algorithm 3: DP-RP-G-OPT-B

- 1 **Input:** Data $u \in [-1, 1]^p$, privacy parameters $\epsilon > 0$, $\delta \in (0, 1)$, number of projections k
 - 2 **Output:** (ϵ, δ) -differentially private random projections $\tilde{x} \in \mathbb{R}^k$
 - 3 Apply RP $x = \frac{1}{\sqrt{k}}W^T u$, where $W \in \mathbb{R}^{p \times k}$ is a random Rademacher matrix
 - 4 Generate iid random noise vector $G \in \mathbb{R}^k$ following $N(0, \sigma^2)$ where σ is obtained by Theorem 3.5 with $\Delta_2 = \beta$
 - 5 Return $\tilde{x} = x + G$
-

Does the reduction in noise magnitude translate into better utility? We first provide an approximate assessment as follows. Note that when the data $u \in [-1, 1]^p$ is not too sparse, the distribution of $\sum_{i=1}^p w_i u_i$, where w_i follows Rademacher distribution, is asymptotically normal according to the Central Limit Theorem (CLT), with mean 0 and variance $\|u\|^2$. This distribution is the same as the distribution of $\sum_{i=1}^p w_i u_i$ when w_i is from $N(0, 1)$. Therefore, we may expect the projected data of Gaussian RP and Rademacher RP to have similar magnitude. Hence, the signal-to-noise ratio (SNR) of DP-RP-G-OPT-B using Rademacher projections would be higher than that of DP-RP-G-OPT using Gaussian projections, as a result of the smaller noise level. An analytical comparison in terms of inner product estimation variance will be given in Section 3.6.

3.5 DP-OPORP: A More Efficient Alternative

The standard random projection (1) requires k projections which takes $O(kp)$ complexity. We can reduce the cost to $O(p)$ by the idea of “binning + RP”. Basically, we split the data entries into k bins, and apply RP in each bin to generate k samples. Zhao et al. (2022) studied noise injection mechanism for count-sketch. Recently, Li and Li (2023a) proposed OPORP (One Permutation +

One Random Projection), an improved variant of count-sketch (Charikar et al., 2004), by using fixed-length binning and normalization. The steps of OPORP for a data vector u are summarized in Algorithm 4 (for convenience, assume p can be integer divided by k).

Algorithm 4: OPORP: count-sketch with fixed-length binning and normalization.

- 1 **Input:** Data vector $u \in \mathbb{R}^p$, number of projected samples k
 - 2 **Output:** k OPORP samples
 - 3 Apply a permutation $\Pi : [p] \mapsto [p]$ to u to get u_Π
 - 4 Split the p permuted data columns (features) into k consecutive fixed-length bins each containing p/k features: $u_\Pi = [u_\Pi^{(1)}, \dots, u_\Pi^{(k)}]$
 - 5 Generate one projection vector $w \in \mathbb{R}^p$ following a proper probability distribution (see Section 3.4). Denote it as a concatenation of bins $w = [w^{(1)}, \dots, w^{(k)}]$
 - 6 Return k projected samples by $x_i = w^{(i)T} u_\Pi^{(i)}$, for $i = 1, \dots, k$.
-

Note that the same permutation Π and projection vector w should be used to process all the data vectors. Let x_i be an OPORP of u , and y_i be an OPORP of v . It can be shown that $\mathbb{E}[x_i y_i] = u^T v$, i.e., OPORP provides an unbiased estimator of the inner product. Regarding the estimation variance, note that in step 2, OPORP deploys a fixed-length binning scheme; in prior works, the lengths of the bins are random and follow a multinomial distribution. Li and Li (2023a) showed that fixed-length binning can reduce the inner product and cosine estimation variance of variable-length binning, by a factor of $\frac{p-k}{p-1}$, when the projection vector follows the symmetric Bernoulli (Rademacher) distribution (see (10)). Furthermore, the estimation variance can be substantially reduced by normalizing the output vector of OPORP. It was also shown by Li and Li (2023a) that one can substantially improve the estimates of “very sparse random projections” via the same normalization technique.

Next, we consider the differential privacy of OPORP and propose DP-OPORP analogously, as given in Algorithm 5. Since we have shown that Gaussian noise would be better than Laplace noise in most cases for DP-SignRP (see Section 3.3), we present the optimal Gaussian noise mechanism here for conciseness. Also, while one may choose any projection vector w in OPORP (Algorithm 4), Li and Li (2023a) showed that the Rademacher projection gives the smallest cosine and inner product estimation variance. Hence, we adopt the Rademacher projection in DP-OPORP.

Algorithm 5: DP-OPORP

- 1 **Input:** Data $u \in [-1, 1]^p$, privacy parameters $\epsilon > 0$, $\delta \in (0, 1)$, number of projections k
 - 2 **Output:** Differentially private OPORP
 - 3 Apply Algorithm 4 with a random Rademacher projection vector to obtain the OPORP x
 - 4 Set sensitivity $\Delta_2 = \beta$
 - 5 Generate iid random vector $G \in \mathbb{R}^k$ following $N(0, \sigma^2)$ where σ is computed by Theorem 3.5
 - 6 Return $\tilde{x} = x + G$
-

In Algorithm 5, we formalize the DP-OPORP method. It is a variant of DP-RP-G-OPT-B, where Gaussian noise is added to the OPORP. Note that the sensitivity $\Delta_2 = \beta$, due to the nature of OPORP: changing the data u by β (Definition 2.3) would lead to at most β change in x in term of l_2 distance. Note that, if we directly add noise to each dimension of the original data, then the sensitivity by definition $\Delta_2 = \max_{(u, u') \in \mathcal{N}(u)} \|f(u) - f(u')\|_2$ is also β .

3.6 Comparison: Inner Product Estimation

We now analytically compare different DP algorithms, in terms of inner product estimation. Here for simplicity, we assume the data are normalized, i.e., the data vector has l_2 norm equal to 1. In this case, the inner product is also the cosine. The baseline method is the most straightforward: we add optimal Gaussian noise to each dimension of the original data (Raw-data-G-OPT). As mentioned earlier, the sensitivity is also $\Delta_2 = \beta$. This means, when we compare all three methods: Raw-data-G-OPT, DP-RP-G-OPT-B, and DP-OPORP, the noise level σ is the same. This makes it convenient to conduct the comparisons, from which we can gain valuable insights.

Theorem 3.8 (Raw-data-G-OPT, i.e., adding optimal Gaussian noise on raw data). *Let σ be the solution to (9) with $\Delta_2 = \beta$. For any $u, v \in \mathcal{U}$, let $\tilde{u}_i = u_i + a_i$ and $\tilde{v}_i = v_i + b_i$ be the DP noisy vectors, with $a_i, b_i \sim N(0, \sigma^2)$ i.i.d. Then, denote $\hat{g}_{org} = \sum_{i=1}^p \tilde{u}_i \tilde{v}_i$. we have*

$$\mathbb{E}[\hat{g}_{org}] = \sum_{i=1}^p u_i v_i, \quad \text{Var}(\hat{g}_{org}) = \sigma^2 \sum_{i=1}^p (u_i^2 + v_i^2) + p\sigma^4. \quad (11)$$

Proof. To add Gaussian noise to the original data, it suffices to find the sensitivity, which, by Definition 2.3, is $\Delta_2 = \beta$. Thus, the approach is (ϵ, δ) -DP according to the optimal Gaussian mechanism (Theorem 3.5). To compute the mean and variance, consider some $i \in [p]$. We have

$$\mathbb{E}[(u_i + a_i)(v_i + b_i)] = \mathbb{E}[u_i v_i + a_i v_i + b_i u_i + a_i b_i] = u_i v_i.$$

Thus, taking the sum implies $\mathbb{E}[\hat{g}_{org}] = \sum_{i=1}^p u_i v_i$. For the variance,

$$\mathbb{E}[(u_i + a_i)(v_i + b_i)]^2 = \mathbb{E}[u_i v_i + a_i v_i + b_i u_i + a_i b_i]^2 = u_i^2 v_i^2 + \sigma^2 (u_i^2 + v_i^2) + \sigma^4,$$

which leads to

$$\text{Var}((u_i + a_i)(v_i + b_i)) = \sigma^2 (u_i^2 + v_i^2) + \sigma^4.$$

Therefore, by independence,

$$\text{Var}(\hat{g}_{org}) = \text{Var}\left(\sum_{i=1}^p (u_i + a_i)(v_i + b_i)\right) = \sigma^2 \sum_{i=1}^p (u_i^2 + v_i^2) + p\sigma^4,$$

which proves the claim. \square

For DP-RP-G-OPT-B and DP-OPORP, we have the following results.

Theorem 3.9 (DP-RP-G-OPT-B inner product estimation). *Let σ be the solution to (9) with $\Delta_2 = \beta$. In Algorithm 3, let $W \in \{-1, 1\}^{p \times k}$ be a Rademacher random matrix. Denote $x = \frac{1}{\sqrt{k}} W^T u$, $y = \frac{1}{\sqrt{k}} W^T v$, and a, b are two random Gaussian noise vectors following $N(0, \sigma^2)$. Let $\hat{g}_{rp} = \sum_{j=1}^k (x_j + a_j)(y_j + b_j)$. Then, $\mathbb{E}[\hat{g}_{rp}] = \sum_{i=1}^p u_i v_i$, and*

$$\text{Var}(\hat{g}_{rp}) = \sigma^2 \sum_{i=1}^p (u_i^2 + v_i^2) + k\sigma^4 + \frac{1}{k} \left(\sum_{i=1}^p u_i^2 \sum_{i=1}^p v_i^2 + \left(\sum_{i=1}^p u_i v_i \right)^2 - 2 \sum_{i=1}^p u_i^2 v_i^2 \right). \quad (12)$$

Proof. The conditional mean and variance can be computed as

$$\mathbb{E} \left[\sum_{j=1}^k (x_j + a_j) (y_j + b_j) \mid x_j, y_j, j = 1, \dots, k \right] = \sum_{j=1}^k x_j y_j,$$

$$\text{Var} \left(\sum_{j=1}^k (x_j + a_j) (y_j + b_j) \mid x_j, y_j, j = 1, \dots, k \right) = \sigma^2 \sum_{j=1}^k (x_j^2 + y_j^2) + k\sigma^4,$$

where the variance calculation follows from Theorem 3.8. Hence, we have

$$\begin{aligned} \mathbb{E} \left[\sum_{j=1}^k (x_j + a_j) (y_j + b_j) \right] &= \mathbb{E} \left[\sum_{j=1}^k x_j y_j \right] = \sum_{i=1}^p u_i v_i, \\ \text{Var}(\hat{g}_{rp}) &= \mathbb{E} \left[\sigma^2 \sum_{j=1}^k (x_j^2 + y_j^2) + k\sigma^4 \right] + \text{Var} \left(\sum_{j=1}^k x_j y_j \right) \\ &= \sigma^2 \sum_{i=1}^p (u_i^2 + v_i^2) + k\sigma^4 + \frac{1}{k} \left(\sum_{i=1}^p u_i^2 \sum_{i=1}^p v_i^2 + \left(\sum_{i=1}^p u_i v_i \right)^2 - 2 \sum_{i=1}^p u_i^2 v_i^2 \right). \end{aligned} \quad (13)$$

In the above calculation, the formula of $\text{Var} \left(\sum_{j=1}^k x_j y_j \right)$ is from the result in Li et al. (2006) with $s = 1$ for Rademacher distribution. \square

Theorem 3.10 (DP-OPORP inner product estimation). *Let σ be the solution to (9) with $\Delta_2 = \beta$. Let $w \in \{-1, 1\}^p$ be a Rademacher random vector. In Algorithm 5, let x and y be the OPORP of u and v , and a, b be two random Gaussian noise vectors following $N(0, \sigma^2)$. Denote $\hat{g}_{oporp} = \sum_{j=1}^k (x_j + a_j)(y_j + b_j)$. Then, $\mathbb{E}[\hat{g}_{oporp}] = \sum_{i=1}^p u_i v_i$, and*

$$\text{Var}(\hat{g}_{oporp}) = \sigma^2 \sum_{i=1}^p (u_i^2 + v_i^2) + k\sigma^4 + \frac{1}{k} \left(\sum_{i=1}^p u_i^2 \sum_{i=1}^p v_i^2 + \left(\sum_{i=1}^p u_i v_i \right)^2 - 2 \sum_{i=1}^p u_i^2 v_i^2 \right) \frac{p-k}{p-1}. \quad (14)$$

Proof. The proof is similar to that of Theorem 3.9, with the help of the result in Li and Li (2023a). \square

The variance reduction factor $\frac{p-k}{p-1}$ can be quite beneficial when p is not very large. Also, see Li and Li (2023a) for the normalized estimators for both OPORP and VSRP (very sparse random projections). The normalization steps can substantially reduce the estimation variance.

Comparison. For the convenience of comparison, let us assume that the data are row-normalized, i.e., $\|u\|^2 = 1$ for all $u \in \mathcal{U}$. Let $\rho = \sum_{i=1}^p u_i v_i$. We have

$$\begin{aligned} \text{Var}(\hat{g}_{org}) &= 2\sigma^2 + p\sigma^4, \\ \text{Var}(\hat{g}_{rp}) &= 2\sigma^2 + k\sigma^4 + \frac{1}{k} \left(1 + \rho^2 - 2 \sum_{i=1}^p u_i^2 v_i^2 \right), \\ \text{Var}(\hat{g}_{oporp}) &= 2\sigma^2 + k\sigma^4 + \frac{1}{k} \left(1 + \rho^2 - 2 \sum_{i=1}^p u_i^2 v_i^2 \right) \frac{p-k}{p-1}. \end{aligned}$$

For high-dimensional data (large p), we see that \hat{g}_{rp} and \hat{g}_{oporp} has roughly the same variance, approximately $2\sigma^2 + k\sigma^4 + \frac{1}{k}$. We would like to compare this with $\text{Var}(\hat{g}_{org}) = 2\sigma^2 + p\sigma^4$ the variance for adding noise directly to the original data.

Let's define the ratio of the variances:

$$R = \frac{2\sigma^2 + p\sigma^4}{2\sigma^2 + k\sigma^4 + \frac{1}{k}} \sim \frac{p\sigma^4}{k\sigma^4} = \frac{p}{k} \quad (\text{if } p \text{ is large or } \sigma \text{ is high}) \quad (15)$$

to illustrate the benefit of RP-type algorithms (DP-RP and DP-OPORP) in protecting the privacy of the (high-dimensional) data. If $\frac{p}{k} = 100$, then it is possible that the ratio of the variances can be roughly 100. This would be a huge advantage. Figure 3 plots the ratio R for $p = 1000$ and $p = 10000$ as well as a series of k/p values, with respect to σ .

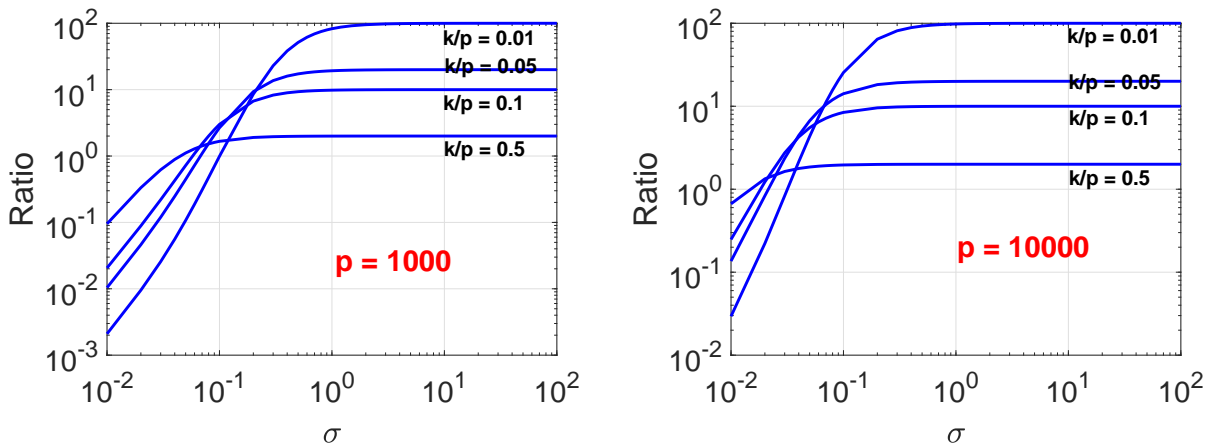


Figure 3: We plot the ratio of variances in (15) for $p = 1000$ and $p = 10000$. We choose k values with $k/p \in \{0.01, 0.05, 0.1, 0.5\}$. Then for any σ value, we are able to compute the ratio R . For larger σ , we have $R \sim \frac{p}{k}$ as expected. See Figure 1 for the relationship among σ , Δ , and ϵ (and δ).

Figure 3 also illustrates when it might be a good strategy to directly add noise to the original data. For example, when $p = 1000$, the ratio can be below 1 if $\sigma < 0.1$. Figure 1 depicts the relationship among σ , Δ , and ϵ (and δ). One can verify that, in order for $\sigma < 0.1$ at $\Delta_2 = \beta = 1$, we need $\epsilon > 100$. In the literature, many DP applications typically require a much smaller ϵ , such as $\epsilon \in [0.1, 20]$ (e.g., [Haerberlen and Khanna \(2014\)](#); [Kenny et al. \(2021\)](#)).

4 DP-SignRP: Differentially Private Sign Random Projections

We have reviewed in the Introduction the advantage of sign random projections (SignRP) (in terms of storage, communications, and computations). In this section, we propose algorithms that output SignRP with differential privacy guarantees. The straightforward approach is directly taking the signs of DP-RP methods, e.g., from Algorithm 1 or Algorithm 3. By the post-processing property of DP, the resultant signs are also DP. In our study, we focus on algorithms that randomize the signs (bit-vector) of the non-private RPs. That is, we first generate non-private SignRP, and then perturb the bits.

In the following, we first study the DP-SignRP from Gaussian random projections. Then we demonstrate the use of Rademacher projections for improving the performance. Finally, we propose algorithms for DP-SignOPORP and discuss its advantages in terms of privacy protection.

4.1 DP-SignRP-RR by Randomized Response

Algorithm 6: DP-SignRP-RR

- 1 **Input:** Data $u \in [-1, 1]^p$; $\epsilon > 0$, $0 < \delta < 1$, number of projections k , norm lower bound m
 - 2 **Output:** Differentially private sign random projections
 - 3 Apply RP by $x = \frac{1}{\sqrt{k}}W^T u$, where $W \in \mathbb{R}^{p \times k}$ is a random $N(0, 1)$ matrix
 - 4 Let $N_+(m, \delta, k, p)$ be computed as (19) in Proposition 4.5
 - 5 Compute $\tilde{s}_j = \begin{cases} \text{sign}(x_j), & \text{with prob. } \frac{e^{\epsilon'}}{e^{\epsilon'}+1} \\ -\text{sign}(x_j), & \text{with prob. } \frac{1}{e^{\epsilon'}+1} \end{cases}$ for $j = 1, \dots, k$, with $\epsilon' = \epsilon/N_+(m, \delta, k, p)$
 - 6 Return \tilde{s} as the DP-SignRP of u
-

Firstly, we develop a DP algorithm for SignRP based on the classic randomized response (RR) technique (Warner, 1965; Dwork and Roth, 2014) and call it DP-SignRP-RR. As summarized in Algorithm 6, after we apply random projection $x = \frac{1}{\sqrt{k}}W^T u$, we take $s = \text{sign}(x)$. Then, for each s_j , we keep the sign with probability $\frac{e^{\epsilon'}}{e^{\epsilon'}+1}$ and flip the sign with probability $\frac{1}{e^{\epsilon'}+1}$. Here $\epsilon' = \epsilon/N_+$, where $N_+(m, \delta, k, p)$ is an upper bound on the number of different signs (among k signs) of $x = \frac{1}{\sqrt{k}}W^T u$ and $x = \frac{1}{\sqrt{k}}W^T u'$ for any β -adjacent (u, u') , which will be derived later in Proposition 4.5. The final output is \tilde{s} after perturbing s by the above procedure. Note that, in Algorithm 6, in order to achieve differential privacy, we additionally assume that there exists a lower bound on the l_2 norm of the data, i.e., $\|u\| \geq m$ for all u in the data domain. We have the following privacy guarantee as a Theorem.

Theorem 4.1. *Algorithm 6 is (ϵ, δ) -DP.*

Remark 4.1. *If we do not assume a lower bound on the data norm (i.e., $m = 0$), then $N_+ = k$. That is, we need to set $\epsilon' = \epsilon/k$ in Algorithm 6, and the algorithm becomes ϵ -DP.*

Proof. For any data point $u \in \mathcal{U}$ and its β -adjacent neighbor u' , denote $s = \text{sign}(W^T u) \in \{-1, +1\}^k$, $s' = \text{sign}(W^T u') \in \{-1, +1\}^k$, and let \tilde{s} and \tilde{s}' be the corresponding randomized sign vectors output by Algorithm 6. Denote $S = \{i : s_i \neq s'_i\}$ and $S^c = [k] \setminus S$. For any vector $y \in \{-1, +1\}^k$, define $S_0 = \{j \in S : s_j = y_j\}$, $S_1 = \{j \in S : s_j \neq y_j\}$, $S_0^c = \{j \in S^c : s_j = y_j\}$ and $S_1^c = \{j \in S^c : s_j \neq y_j\}$.

By Proposition 4.5, we know that the event $\{|S| \leq N_+(m, \delta, k, p)\}$ happens with probability at least $1 - \delta$. In this event, we have

$$\begin{aligned} \log \frac{Pr(\tilde{s} = y)}{Pr(\tilde{s}' = y)} &= \log \frac{\prod_{j \in S_0^c} \frac{e^{\epsilon'}}{e^{\epsilon'} + 1} \prod_{j \in S_1^c} \frac{1}{e^{\epsilon'} + 1} \prod_{j \in S_0} \frac{e^{\epsilon'}}{e^{\epsilon'} + 1} \prod_{j \in S_1} \frac{1}{e^{\epsilon'} + 1}}{\prod_{j \in S_0^c} \frac{e^{\epsilon'}}{e^{\epsilon'} + 1} \prod_{j \in S_1^c} \frac{1}{e^{\epsilon'} + 1} \prod_{j \in S_0} \frac{1}{e^{\epsilon'} + 1} \prod_{j \in S_1} \frac{e^{\epsilon'}}{e^{\epsilon'} + 1}} \\ &\leq \log \frac{\prod_{j \in S} \frac{e^{\epsilon'}}{e^{\epsilon'} + 1}}{\prod_{j \in S} \frac{1}{e^{\epsilon'} + 1}} = |S| \epsilon' \leq N_+ \epsilon' = \epsilon. \end{aligned}$$

Since this event occurs with probability at least $1 - \delta$, the overall procedure is (ϵ, δ) -DP. \square

4.1.1 The flipping probability and calculation of N_+

As in the proof of Theorem 4.1, N_+ is the upper bound on $S = \{i : s_j \neq s'_j\}$, where $s = \text{sign}(W^T u) \in \{-1, +1\}^k$ and $s' = \text{sign}(W^T u') \in \{-1, +1\}^k$ for neighboring data vectors (u, u') . N_+ also determines the flipping probability in DP-SignRP-RR, which is important for the utility. Next, we analyze N_+ . The following is a useful lemma that describes some statistical properties of the absolute value of bivariate normal random variables, which might be of independent interest. The proof can be found in Appendix.

Lemma 4.2. Let $\begin{pmatrix} X \\ Y \end{pmatrix} \sim N \begin{pmatrix} \sigma_x^2 & \rho \sigma_x \sigma_y \\ \rho \sigma_x \sigma_y & \sigma_y^2 \end{pmatrix}$. Denote $r = \sigma_x / \sigma_y$. Then we have:

1. $Pr(|X| > |Y|) = \frac{1}{\pi} \left[\tan^{-1} \left(\frac{r - \rho}{\sqrt{1 - \rho^2}} \right) + \tan^{-1} \left(\frac{r + \rho}{\sqrt{1 - \rho^2}} \right) \right]$. When $r \leq 1$, the maximum is achieved at $\rho = 0$, i.e., $\max_{\rho} Pr(|X| < |Y|) = \frac{2}{\pi} \tan^{-1}(r)$.

2. The conditional expectation:

$$\mathbb{E}[|X| | |X| > |Y|] = \sigma_x \sqrt{\frac{\pi}{2}} \cdot \frac{\frac{r - \rho}{\sqrt{1 + r^2 - 2r\rho}} + \frac{r + \rho}{\sqrt{1 + r^2 + 2r\rho}}}{\tan^{-1} \left(\frac{r - \rho}{\sqrt{1 - \rho^2}} \right) + \tan^{-1} \left(\frac{r + \rho}{\sqrt{1 - \rho^2}} \right)}. \quad (16)$$

3. The conditional tail probability: for any $r > 0$, $\rho \in (-1, 1)$, for any $t > 0$,

$$Pr(|X| > t | |X| > |Y|) \leq \exp \left(-\frac{t^2}{2\sigma_x^2} \right). \quad (17)$$

With Lemma 4.2, we have the following result on the maximum of a group of Gaussian variables.

Lemma 4.3. Let X_1, \dots, X_p be iid $N(0, \sigma_x^2)$ variables. Let $Y \sim N(0, \sigma_y^2)$ be another Gaussian random variable with arbitrary dependence structure with X_i 's. Let $r = \sigma_x / \sigma_y \leq 1$. Then

$$P_+(r, p) := Pr(\max_{i=1, \dots, p} |X_i| > |Y|) \leq \int_0^\infty 2p[2\Phi(t) - 1]^{p-1} [2\Phi(rt) - 1] \phi(t) dt, \quad (18)$$

where $\phi(x)$ and $\Phi(x)$ are the standard Gaussian pdf and cdf, respectively.

Proof. By Lemma 4.2 and independence, we know that $Pr(\max_{i=1, \dots, p} |X_i| > |Y|)$ reaches its maximum when X_i is independent of Y , i.e., when $\rho(X_i, Y) = 0$, $\forall i = 1, \dots, p$. Since $|X_i|$ follows a half-normal distribution with cdf being $\text{erf}(\frac{x}{\sqrt{2}\sigma_x})$, we have

$$Pr(\max_{i=1, \dots, p} |X_i| \leq t) = \text{erf} \left(\frac{t}{\sqrt{2}\sigma_x} \right)^p = \left[2\Phi \left(\frac{x}{\sigma_x} \right) - 1 \right]^p,$$

and probability density function $g(x) = 2p[\Phi(\frac{x}{\sigma_x}) - 1]^{p-1} \frac{1}{\sqrt{2\pi}\sigma_x} e^{-\frac{x^2}{2\sigma_x^2}}$. When Y is independent of all X_i 's (which gives the upper bound), we have

$$\begin{aligned} Pr(\max_{i=1,\dots,p} |X| > |Y|) &= \int_0^\infty 2p \left[\Phi\left(\frac{x}{\sigma_x}\right) - 1 \right]^{p-1} \frac{1}{\sqrt{2\pi}\sigma_x} e^{-\frac{x^2}{2\sigma_x^2}} Pr(|Y| < x) dx \\ &= \int_0^\infty 2p \left[\Phi\left(\frac{x}{\sigma_x}\right) - 1 \right]^{p-1} \frac{1}{\sqrt{2\pi}\sigma_x} e^{-\frac{x^2}{2\sigma_x^2}} \operatorname{erf}\left(\frac{x}{\sqrt{2}\sigma_y}\right) dx \\ &= \int_0^\infty 2p[2\Phi(t) - 1]^{p-1} [2\Phi(rt) - 1] \phi(t) dt, \end{aligned}$$

with a proper change of variables. This gives an upper bound as shown above. \square

In Lemma 4.3, $P_+(r, p)$ is an increasing function in both r and p . In Figure 4, we plot the $P_+(r, p)$ with different r and p values. We see that when r is as small as 0.1, $P_+(r, p)$ is smaller than 0.4 when p is as large as 10^6 .

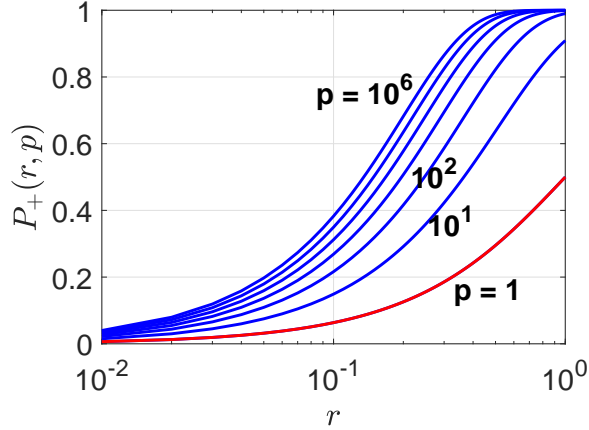


Figure 4: $P(r, p)$ in (18) in Lemma 4.3 against $r \leq 1$ at different p . The red curve ($p = 1$) also equals $Pr(|X| > |Y|)$ in Lemma 4.2.

Equipped with Lemma 4.3, we can bound N_+ in Algorithm 6, the largest number of projected signs that are possible to change when u is replaced by any neighboring data vector u' .

Lemma 4.4 (Binomial tail bound). *Let $X \sim \text{Binomial}(n, p)$ and denote $\mu = \mathbb{E}[X] = np$. For any $\eta > 0$, it holds that*

$$Pr(X \geq (1 + \eta)\mu) \leq \exp\left(-\frac{\eta^2 \mu}{\eta + 2}\right).$$

Proposition 4.5 (Bounding N_+). *Suppose $u \in [-1, 1]^p$ and $\beta \leq \|u\|$. Denote $r = \frac{\beta}{\|u\|}$ and $F_{\|u\|, p} = P_+(\frac{\beta}{\|u\|}, p)$ as (18) in Lemma 4.3. Denote $s = \text{sign}(W^T u) \in \{-1, +1\}^k$ and $s' = \text{sign}(W^T u') \in \{-1, +1\}^k$ for u' that is β -neighboring to u , and $S = \{i : s_j \neq s'_j\}$. Then, with probability $1 - \delta$,*

$$|S| \leq N_+(\|u\|, \delta, k, p) = \min\left\{F_{\|u\|, p} k + \frac{1}{2} \left[\log(1/\delta) + \sqrt{(\log(1/\delta))^2 + 8F_{\|u\|, p} k \log(1/\delta)} \right], k\right\}. \quad (19)$$

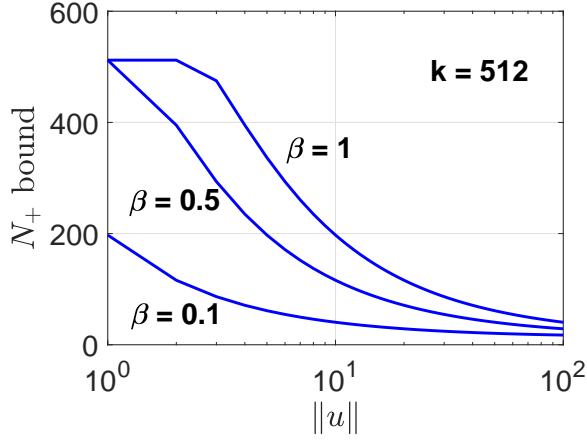


Figure 5: The upper bound on $N_+(\|u\|, \delta, k, p)$ in Proposition 4.5 against data norm $\|u\|$ at different β . In the simulation, $p = 1024$, $k = 512$ and $\delta = 10^{-6}$.

Remark 4.2. Since $F_{\|u\|,p} = P_+(r, p)$ is an increasing function in $r = \beta/\|u\|$, N_+ would be smaller if $\beta/\|u\|$ is smaller. That is, the signs of $W^T u$ and $W^T u'$ are less likely to be different when the difference between neighboring data, β , is relatively small compared with the data norm $\|u\|$.

Proof. Consider a single Gaussian projection vector w with iid $N(0,1)$ entries. Since $w^T u = \sum_{i=1}^p u_i w_i$ and each $w_i \sim N(0,1)$, we know that $\begin{pmatrix} \beta w_i \\ x \end{pmatrix} \sim N\left(\begin{matrix} \beta^2 & \rho_i \beta \|u\| \\ \rho_i \beta \|u\| & \|u\|^2 \end{matrix}\right)$ where $\rho_i = \frac{u_i}{\|u\|}$ is the correlation coefficient. Since $|w^T(u - u')| \leq \beta \max_{i=1,\dots,p} |w_i|$ by Definition 2.3 of β -neighboring (and more generally, when $\|u - u'\|_1 \leq \beta$), we have

$$Pr\left(\max_{u' \in Nb(u)} |w^T(u - u')| \geq |w^T u|\right) = Pr\left(\beta \max_{i=1,\dots,p} |w_i| \geq |w^T u|\right).$$

Note that, $\beta \max_{i=1,\dots,p} |w_i| \geq |w^T u|$ is a necessary condition for the event that there exists a neighbor such that $\text{sign}(w^T u) \neq \text{sign}(w^T u')$. Denote $I = \mathbb{1}\{\beta \max_{i=1,\dots,p} |w_i| \geq |w^T u|\}$. Applying Lemma 4.3 with $r = \beta/\|u\| \leq 1$ yields

$$\mathbb{E}[I] = Pr\left(\beta \max_{i=1,\dots,p} |w_i| \geq |w^T u|\right) \leq F_{\|u\|,p} = \int_0^\infty 2p[2\Phi(t) - 1]^{p-1}[2\Phi(rt) - 1]\phi(t)dt \quad (20)$$

as given by (18). Let I_j be the corresponding indicator function w.r.t. each column in the projection matrix W . Denote $N_+ = \sum_{j=1}^k I_j$, and by the above reasoning, we know that $|S| \leq N_+$ where S is defined in the theorem. Since the columns of W are independent, N_+ follows a *Binomial*($k, \mathbb{E}[I]$) distribution with k trials and success probability $\mathbb{E}[I]$ bounded as above. Applying Chernoff's bound on binomial variable (Lemma 4.4), we obtain

$$Pr(N_+ \geq (1 + \eta)F_{\|u\|,p}k) \leq \exp\left(-\frac{\eta^2 F_{\|u\|,p}k}{\eta + 2}\right).$$

Setting the RHS to δ gives $\eta = \frac{\log(1/\delta) + \sqrt{(\log(1/\delta))^2 + 8F_{\|u\|,p}k \log(1/\delta)}}{2F_{\|u\|,p}k}$. Therefore, with probability $1 - \delta$,

$$N_+(\|u\|, \delta, k, p) \leq F_{\|u\|,p}k + \frac{1}{2} \left[\log(1/\delta) + \sqrt{(\log(1/\delta))^2 + 8F_{\|u\|,p}k \log(1/\delta)} \right].$$

In addition, $N_+ \leq k$ trivially. The proof is complete. \square

In Figure 5, we plot the bound on $N_+(\|u\|, \delta, k, p)$ derived in Proposition 4.5 against $\|u\|$ with various β and fixed p, k and δ . As expected, $N_+(\|u\|, \delta, k, p)$ shrinks rapidly as the data norm $\|u\|$ increases. Since $N_+(\|u\|, \delta, k, p)$ is decreasing in $\|u\|$ (because $F_{\|u\|, p}$ decreases with $\|u\|$), we know that for all u with $\|u\| \geq m$, the $|S|$ in Proposition 4.5 would be upper bounded by $N_+(m, \delta, k, p)$ with high probability, as used in Algorithm 6 and the proof of Theorem 4.1. Also, in DP-SignRP-RR, the probability of flipping the true SignRP, $\frac{1}{e^{\epsilon/N_++1}}$, would be smaller when the data norm (or, its lower bound m) is large compared with β .

4.1.2 Utility in angle estimation by DP-SignRP-RR

Define the DP-SignRP-RR estimator of the angle between two data points u and v as

$$\hat{\theta}_{RR} = \pi(1 - \hat{P}_{RR}), \quad (21)$$

$$\text{where } \hat{P}_{RR} = \frac{(e^{\epsilon'} + 1)^2}{(e^{\epsilon'} - 1)^2} \frac{1}{k} \sum_{j=1}^k \mathbb{1}\{\tilde{s}_{1j} = \tilde{s}_{2j}\} - \frac{2e^{\epsilon'}}{(e^{\epsilon'} - 1)^2}.$$

We have the following result on the utility.

Theorem 4.6. *Let $\rho = \cos(u, v)$ and $\theta = \cos^{-1}(\rho)$. Run Algorithm 6 with N_+ given in Proposition 4.5 and define the DP-SignRP-RR angle estimator by (21). We have $\mathbb{E}[\hat{\theta}_{RR}] = \theta$. As $k \rightarrow \infty$, the following holds:*

$$\hat{\theta}_{RR} \rightarrow N\left(\theta, \frac{V_{RR}}{k}\right),$$

where

$$V_{RR} = \theta(\pi - \theta) + \frac{2\pi^2 e^{\epsilon/N_+}}{(e^{\epsilon/N_+} - 1)^2} + \frac{4\pi^2 e^{2\epsilon/N_+}}{(e^{\epsilon/N_+} - 1)^4}.$$

Proof. Let $s = \text{sign}(W^T u) \in \{-1, +1\}^k$, $s' = \text{sign}(W^T u') \in \{-1, +1\}^k$. We denote the collision probability of non-private SignRP as

$$P_{SRP} = \Pr(s_{1j} = s_{2j}) = 1 - \frac{\cos^{-1}(\rho)}{\pi} = 1 - \frac{\theta}{\pi}.$$

Hence, the collision probability of DP-SignRP-RR can be computed as

$$\begin{aligned} \tilde{P} &:= \Pr(\tilde{s}_{1j} = \tilde{s}_{2j}) = \Pr(s_{1j} = s_{2j}, \text{ both change sign or not change sign}) \\ &\quad + \Pr(s_{1j} \neq s_{2j}, \text{ one sign changes}) \\ &= P_{SRP} \left[\left(\frac{e^{\epsilon'}}{e^{\epsilon'} + 1}\right)^2 + \left(\frac{1}{e^{\epsilon'} + 1}\right)^2 \right] + 2(1 - P_{SRP}) \frac{e^{\epsilon'}}{(e^{\epsilon'} + 1)^2} \\ &= P_{SRP} \frac{(e^{\epsilon'} - 1)^2}{(e^{\epsilon'} + 1)^2} + \frac{2e^{\epsilon'}}{(e^{\epsilon'} + 1)^2}, \end{aligned}$$

which increases linearly in P_{SRP} . Thus, it holds that

$$\mathbb{E}[\hat{P}_{RR}] = \frac{(e^{\epsilon'} + 1)^2}{(e^{\epsilon'} - 1)^2} \tilde{P} - \frac{2e^{\epsilon'}}{(e^{\epsilon'} - 1)^2} = P_{SRP} = 1 - \frac{\theta}{\pi},$$

which implies $\mathbb{E}[\hat{\theta}_{RR}] = \pi(1 - (1 - \frac{\theta}{\pi})) = \theta$. To compute the variance, we first estimate $\theta = \cos^{-1}(\rho)$ by

$$\hat{\theta} = \pi(1 - \hat{P}_{RR}).$$

Then according to the Central Limit Theorem (CLT), for the sample mean of iid Bernoulli's, as $k \rightarrow \infty$, we have

$$\frac{1}{k} \sum_{j=1}^k \mathbb{1}\{\tilde{s}_{1j} = \tilde{s}_{2j}\} \rightarrow N(\tilde{P}, \frac{\tilde{P}(1 - \tilde{P})}{k}).$$

As a result, we have $\hat{\theta} \rightarrow N(\theta, \frac{V_{RR}}{k})$, where

$$\begin{aligned} V_{RR} &= \frac{\pi^2(e^{\epsilon'} + 1)^4}{(e^{\epsilon'} - 1)^4} \left[\left(1 - \frac{\theta}{\pi}\right) \frac{(e^{\epsilon'} - 1)^2}{(e^{\epsilon'} + 1)^2} + \frac{2e^{\epsilon'}}{(e^{\epsilon'} + 1)^2} \right] \left[\frac{e^{2\epsilon'} + 1}{(e^{\epsilon'} + 1)^2} - \left(1 - \frac{\theta}{\pi}\right) \frac{(e^{\epsilon'} - 1)^2}{(e^{\epsilon'} + 1)^2} \right] \\ &= \frac{\pi^2(e^{\epsilon'} + 1)^4}{(e^{\epsilon'} - 1)^4} \left[\left(1 - \frac{\theta}{\pi}\right) \frac{(e^{\epsilon'} - 1)^2}{(e^{\epsilon'} + 1)^2} + \frac{2e^{\epsilon'}}{(e^{\epsilon'} + 1)^2} \right] \left[\frac{\theta}{\pi} \frac{(e^{\epsilon'} - 1)^2}{(e^{\epsilon'} + 1)^2} + \frac{2e^{\epsilon'}}{(e^{\epsilon'} + 1)^2} \right] \\ &= \frac{\pi^2\theta}{\pi} \left(1 - \frac{\theta}{\pi}\right) + \left(1 - \frac{\theta}{\pi}\right) \frac{2e^{\epsilon'}}{(e^{\epsilon'} - 1)^2} + \frac{\theta}{\pi} \frac{2e^{\epsilon'}}{(e^{\epsilon'} - 1)^2} + \frac{4e^{2\epsilon'}}{(e^{\epsilon'} - 1)^4} \\ &= \theta(\pi - \theta) + \frac{2\pi^2 e^{\epsilon'}}{(e^{\epsilon'} - 1)^2} + \frac{4\pi^2 e^{2\epsilon'}}{(e^{\epsilon'} - 1)^4}. \end{aligned}$$

We conclude the proof by replacing $\epsilon' = \epsilon/N_+$. □

Theorem 4.6 says that $\hat{\theta}_{RR}$ is an unbiased estimator of θ and asymptotically normal. Compared with the variance in (5) of the estimator from SignRP, we see that $\hat{\theta}_{RR}$ incurs an extra variance (i.e., utility loss) of $\frac{\pi^2}{k} \left[\frac{2e^{\epsilon/N_+}}{(e^{\epsilon/N_+} - 1)^2} + \frac{4e^{2\epsilon/N_+}}{(e^{\epsilon/N_+} - 1)^4} \right]$. This quantity increases as ϵ gets smaller, illustrating the utility-privacy trade-off of DP-SignRP-RR.

Optimal projection dimension k^* . In Theorem 4.6, note that the variance V_{RR} does not always decrease with larger k . In particular, in Proposition 4.5 since $N_+ \asymp F_{\|u\|,p} k$, the term $\left[\frac{2e^{\epsilon/N_+}}{(e^{\epsilon/N_+} - 1)^2} + \frac{4e^{2\epsilon/N_+}}{(e^{\epsilon/N_+} - 1)^4} \right]$ increases with k . Therefore, there exists an optimal k^* that minimizes the estimation variance. When k is sufficiently large, we have the approximation

$$\frac{V_{RR}}{k} \approx \frac{\theta(\pi - \theta)}{k} + \frac{2\pi^2 F_{\|u\|,p}^2 k}{\epsilon^2} + \frac{8\pi^2 F_{\|u\|,p}^4 k^3}{\epsilon^4},$$

using the approximation that $e^x - 1 \approx x$ when x is small. To find the optimal k minimizing this expression, we compute the derivative and set it as zero:

$$-\frac{\theta(\pi - \theta)}{k^2} + \frac{2\pi^2 F_{\|u\|,p}^2}{\epsilon^2} + \frac{24\pi^2 F_{\|u\|,p}^4 k^2}{\epsilon^4} = 0 \implies k^* \asymp \frac{\epsilon\theta(\pi - \theta)}{F_{\|u\|,p}}.$$

This analysis suggests that theoretically the optimal k^* is larger when: (1) ϵ is large; (2) $F_{\|u\|,p}$ is small, which is typically true when the norm of the data is relatively large.

4.2 DP-SignRP-RR-Smooth Using Smooth Flipping Probability

The DP-SignRP-RR algorithm is not satisfactory in terms of privacy preservation. For instance, when the norm of the data is not very large (e.g., $m = 10$ and $\beta = 1$), for $k = 512$, N_+ can be as large as 200 (see Figure 5). This implies that, we need $\epsilon = 400$ in order for the probability of flipping a true SignRP to be $\frac{1}{e^{\epsilon/N_+} + 1} \approx 11.9\%$, which is still fairly large to achieve a good utility in practice. Thus, the privacy protection of DP-SignRP-RR might be too weak. Next, we develop a new algorithm that could reduce the flipping probability of DP-SignRP-RR, thanks to the “robustness” of SignRP brought by the “aggregate-and-sign” operation.

Algorithm 7: DP-SignRP-RR-smooth using smooth flipping probability

- 1 **Input:** Data $u \in [-1, 1]^p$; $\epsilon > 0$, number of projections k
 - 2 **Output:** Differentially private sign random projections
 - 3 Apply RP by $x = \frac{1}{\sqrt{k}} W^T u$, where $W \in \mathbb{R}^{p \times k}$ is a random $N(0, 1)$ matrix
 - 4 Compute $L_j = \lceil \frac{|x_j|}{\beta \max_{i=1, \dots, p} |W_{ij}|} \rceil$ for $j = 1, \dots, k$
 - 5 Compute $\tilde{s}_j = \begin{cases} \text{sign}(x_j), & \text{with prob. } \frac{e^{\epsilon'_j}}{e^{\epsilon'_j} + 1} \\ -\text{sign}(x_j), & \text{with prob. } \frac{1}{e^{\epsilon'_j} + 1} \end{cases}$ for $j = 1, \dots, k$, with $\epsilon'_j = \frac{L_j}{k} \epsilon$
 - 6 Return \tilde{s} as the DP-SignRP of u
-

Smooth flipping probability. We propose a novel sampling approach based on “smooth flipping probability”. Recall the motivation of smooth sensitivity (Definition 2.5): we may allow the use of local sensitivity at u as long as we account for the local sensitivities of all $u' \in \mathcal{U}$, discounted exponentially by a factor $e^{-\epsilon d(u, u')}$ where $d(u, u')$ is the minimal number of “taking-a-neighbor” operations to reach u' from u . Conceptually, smooth sensitivity says that, the farther u is from a high local sensitivity point, the less noise is needed for u to achieve DP.

What is the “local perturbation” for the 1-bit SignRP? Consider one projection $x_j = W[:, j]^T u$ and $s_j = \text{sign}(x_j)$. For a neighbor u' of u , denote $x'_j = W[:, j]^T u'$ and $s'_j = \text{sign}(x'_j)$. Obviously, by β -adjacency (Definition 2.3), s'_j is possible to be different from s_j only if $|x_j| < \beta \max_{i=1, \dots, p} |W_{ij}|$, because $|x_j - x'_j| \leq \beta \max_{i=1, \dots, p} |W_{ij}|$. Intuitively, this implies that projected values near zero would have larger “local sensitivity”. More concretely,

- When $|x_j| < \beta \max_{i=1, \dots, p} |W_{ij}|$, the “local sign flipping” (analogue to the local sensitivity for noise addition) is required, since s'_j may change the sign of s_j . A typical choice is the standard randomized response (RR) strategy: keep the sign with probability $\frac{e^{\epsilon/k}}{e^{\epsilon/k} + 1}$ and flip otherwise.
- When $|x_j| \geq \beta \max_{i=1, \dots, p} |W_{ij}|$, there does not exist $u' \in Nb(u)$ such that $s'_j \neq s_j$. Thus, the “local sign flipping” is not needed (i.e., locally, we do not need to apply random sign flips). However, due to the same issue as the local sensitivity, if we do not perturb s_j in this case, then the algorithm does not satisfy DP. Instead, we leverage the idea of smooth sensitivity and propose “smooth flipping probability” which applies less perturbation for points far away from the “high-sensitivity region” (i.e., the regime with $|x_j| < \beta \max_{i=1, \dots, p} |W_{ij}|$). Specifically, we define $L_j = \lceil \frac{|x_j|}{\beta \max_{i=1, \dots, p} |W_{ij}|} \rceil$. The probability of keeping the sign s_j is $P_j^{(u)} = \frac{e^{\epsilon'_j}}{e^{\epsilon'_j} + 1}$ where $\epsilon'_j = \frac{L_j}{k} \epsilon$. In Theorem 4.7, we will see that this flipping probability is “smooth”: for $\forall u, u'$ that are neighbors, $P_j^{(u)} \leq e^{\epsilon/k} P_j^{(u')}$, which justifies its name.

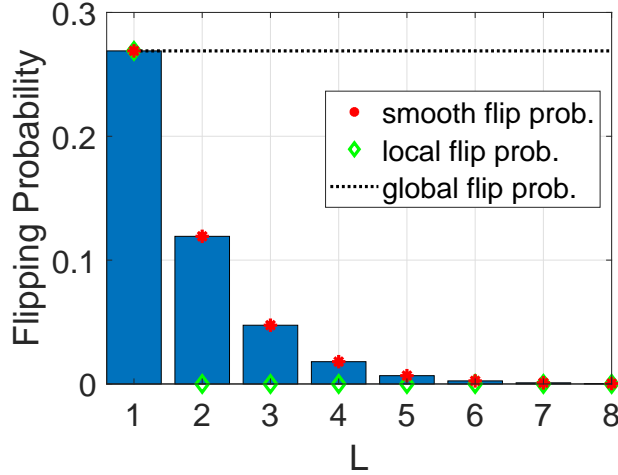


Figure 6: Illustration of the smooth flipping probability, “local flipping probability”, and the global upper bound for DP-SignRP. $\epsilon = 1$, $k = 1$. L is computed in Algorithm 7.

The concrete steps of DP-SignRP-RR-smooth are summarized in Algorithm 7. Note that, the above two cases can be unified into one, since the first case corresponds to $L_j = 1$ which exactly recovers the flipping probability $\frac{e^{\epsilon/k}}{e^{\epsilon/k} + 1}$. In Figure 6, we provide an illustrative example of the smooth flipping probability (red) and the “local flipping probability” (green) discussed above. We see that the local flipping probability is only non-zero at $L = 1$, i.e., when s_j and s'_j are possible to be different. The proposed smooth flipping probability is non-zero for all $L > 0$, but keeps shrinking as L is larger, i.e., as the projected value is farther from 0.

Theorem 4.7. *Algorithm 7 is ϵ -DP.*

Proof. Let us consider a single projection vector $w_j = W_{[:,j]}$. Denote $x_j = w_j^T u$ and $x'_j = w_j^T u'$ for a neighboring data u' of u , and $s_j = \text{sign}(x_j)$, $s'_j = \text{sign}(x'_j)$. Also, let $L_j = \lceil \frac{|x_j|}{\beta \max_{i=1, \dots, p} |W_{ij}|} \rceil$ and $L'_j = \lceil \frac{|x'_j|}{\beta \max_{i=1, \dots, p} |W_{ij}|} \rceil$. W.l.o.g., we can assume $s_j = 1$ by the symmetry of random projection and the symmetry of DP. Consider two cases:

- Case I: $L_j \geq 2$. In this case, we know that $s'_j = s_j$, i.e., the change from u to u' will not change the sign of the projection. Thus, in Algorithm 7, we have

$$\frac{\Pr(\tilde{s}_j = 1)}{\Pr(\tilde{s}'_j = 1)} = \exp\left(\frac{L_j - L'_j}{k} \epsilon\right) \frac{\exp\left(\frac{L'_j}{k} \epsilon\right) + 1}{\exp\left(\frac{L_j}{k} \epsilon\right) + 1}.$$

By the definition of β -adjacency, $|L_j - L'_j|$ equals either 0 or 1. When $L_j = L'_j$, $\frac{\Pr(\tilde{s}_j = 1)}{\Pr(\tilde{s}'_j = 1)} = 1$. When $L_j - L'_j = 1$, we have

$$\frac{\Pr(\tilde{s}_j = 1)}{\Pr(\tilde{s}'_j = 1)} = \frac{\exp\left(\frac{L_j}{k} \epsilon\right) + \exp\left(\frac{1}{k} \epsilon\right)}{\exp\left(\frac{L_j}{k} \epsilon\right) + 1}.$$

Hence, we have $1 \leq \frac{\Pr(\tilde{s}_j = 1)}{\Pr(\tilde{s}'_j = 1)} \leq e^{\frac{\epsilon}{k}}$ by the numeric identity $1 \leq \frac{a+c}{b+c} \leq \frac{a}{b}$ for $a \geq b > 0$ and

$c > 0$. Thus, by symmetry, $e^{-\frac{\epsilon}{k}} \leq \frac{Pr(\tilde{s}_j=1)}{Pr(\tilde{s}'_j=1)} \leq e^{\frac{\epsilon}{k}}$. On the other hand,

$$\frac{Pr(\tilde{s}_j = -1)}{Pr(\tilde{s}'_j = -1)} = \frac{\exp(\frac{L'_j}{k}\epsilon) + 1}{\exp(\frac{L_j}{k}\epsilon) + 1}.$$

Similarly, when $L_j = L'_j$, the ratio equals 1. When $L_j = L'_j - 1$, we have $\frac{Pr(\tilde{s}_j=-1)}{Pr(\tilde{s}'_j=-1)} \leq \exp(\frac{L'_j}{k}\epsilon - \frac{L_j}{k}\epsilon) = e^{\frac{\epsilon}{k}}$. By symmetry we obtain $e^{-\frac{\epsilon}{k}} \leq \frac{Pr(\tilde{s}_j=-1)}{Pr(\tilde{s}'_j=-1)} \leq e^{\frac{\epsilon}{k}}$.

- Case II: $L_j = 1$. In this case, s_j might be different from s'_j . First, if $L'_j = 2$, then the above analysis also applies that $\frac{Pr(\tilde{s}_j=1)}{Pr(\tilde{s}'_j=1)}$ and $\frac{Pr(\tilde{s}_j=-1)}{Pr(\tilde{s}'_j=-1)}$ are both lower and upper bounded by $e^{-\frac{\epsilon}{k}}$ and $e^{\frac{\epsilon}{k}}$, respectively. It suffices to examine the case when $L'_j = 1$. In this case, if $s'_j = s_j = 1$ then the probability ratios simply equal 1. If $s'_j = -1$, we have

$$\frac{Pr(\tilde{s}_j = 1)}{Pr(\tilde{s}'_j = 1)} = \frac{\frac{\exp(\frac{\epsilon}{k})}{\exp(\frac{\epsilon}{k})+1}}{\frac{1}{\exp(\frac{\epsilon}{k})+1}} = e^{\frac{\epsilon}{k}}, \quad \frac{Pr(\tilde{s}_j = -1)}{Pr(\tilde{s}'_j = -1)} = \frac{\frac{1}{\exp(\frac{\epsilon}{k})+1}}{\frac{\exp(\frac{\epsilon}{k})}{\exp(\frac{\epsilon}{k})+1}} = e^{-\frac{\epsilon}{k}}.$$

Combining two cases, we have that $\log \frac{Pr(\tilde{s}_j=t)}{Pr(\tilde{s}'_j=t)} \leq \frac{\epsilon}{k}$, for $t = -1, 1$, and for all $j = 1, \dots, k$. That is, each single perturbed sign achieves $\frac{\epsilon}{k}$ -DP. Since the k projections are independent, by Theorem 2.3, we know that the output bit vector $\tilde{s} = [\tilde{s}_1, \dots, \tilde{s}_k]$ is ϵ -DP as claimed. \square

Comparison with DP-SignRP-RR (Algorithm 6). In terms of algorithm design and privacy, DP-SignRP-RR-smooth (Algorithm 7) has the following two advantages over the standard DP-SignRP-RR method (Algorithm 6):

1. DP-SignRP-RR-smooth does not require (assume) a lower bound m on the data norms;
2. DP-SignRP-RR-smooth achieves ϵ -DP, while DP-SignRP-RR can only guarantee (ϵ, δ) -DP.

Regarding the second point, as mentioned in Remark 4.1, Algorithm 6 can also achieve ϵ -DP if we set the flipping probability to be $\frac{1}{e^{\epsilon/k}+1}$. Note that this equals the flipping probability in Algorithm 7 when $L_j = 1$, which is the “worst” global bound on the flipping probability. In many cases, a good proportion of L_j $j = 1, \dots, k$ would be greater than 1. Therefore, when both are ϵ -DP, DP-SignRP-RR-smooth requires a much smaller flipping probability than DP-SignRP-RR.

4.3 DP-SignRP with Rademacher Projections

At this point, it should be clear that the flipping probability of DP-SignRP (both DP-SignRP-RR and DP-SignRP-RR-smooth) essentially depends on how concentrated the projected data is around zero. Particularly, N_+ in Algorithm 6, as given in Proposition 4.5, is a high probability upper bound on a Binomial random variable with success probability $Pr(\beta \max_{i=1, \dots, p} |w_i| \geq |w^T u|)$ with $w \sim N(0, 1)$. In Algorithm 7, $L_j = \lceil \frac{|w_j^T u|}{\beta \max_{i=1, \dots, p} |w_{ij}|} \rceil$. For both quantities, a smaller value leads to a smaller sign flipping probability and thus better utility.

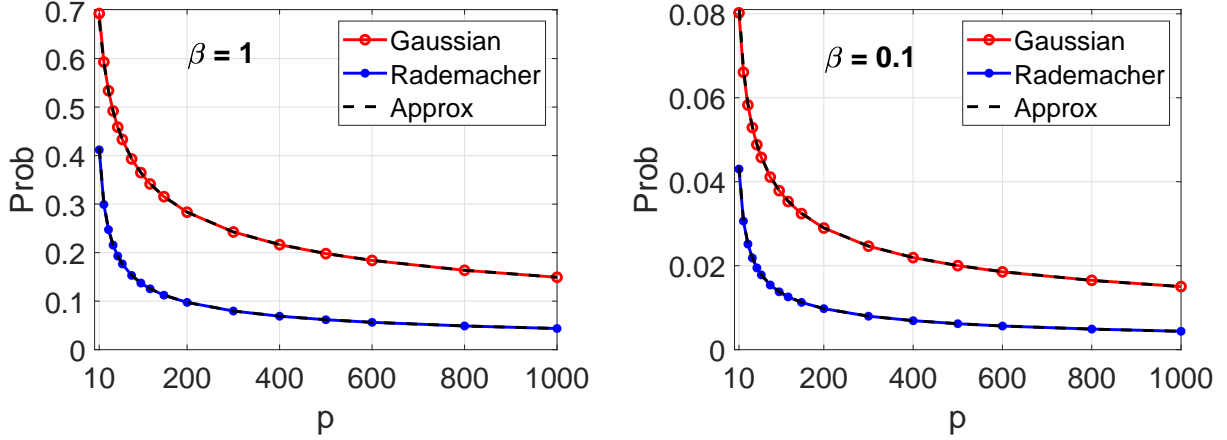


Figure 7: Simulations for evaluating (23) and (24), using two choices for w : the Gaussian distribution and the Rademacher distribution (i.e., (10) with $s = 1$). We plot the two upper bounds (23) and (24) as black dashed curves, which essentially both overlap with their corresponding simulations.

N_+ in **DP-SignRP-RR**. We first consider the N_+ in Algorithm 6, which determines the flipping probability $\frac{1}{e^{\epsilon/N_+} + 1}$. Particularly, N_+ in Algorithm 6, as given in Proposition 4.5, is a high probability upper bound on a Binomial random variable with success probability

$$P_+ = Pr \left(\beta \max_{i=1, \dots, p} |w_i| \geq |w^T u| \right), \quad (22)$$

where w is the p -dimensional projection vector. When w_i is sampled from the Rademacher distribution, i.e., $w_i \in \{-1, +1\}$ with equal probabilities, the probability calculation can be simplified:

$$P_{+,b} = Pr \left(\beta \max_{i=1, \dots, p} |w_i| \geq \left| \sum_{i=1}^p w_i u_i \right| \right) = Pr \left(\beta \geq \left| \sum_{i=1}^p w_i u_i \right| \right) \approx 2\Phi \left(\frac{\beta}{\|u\|} \right) - 1. \quad (23)$$

Based on the central limit theorem, the normal approximation (23) is accurate unless p is very small. Recall that, when w_i 's are sampled from the Gaussian distribution, we have already calculated an upper bound in (20), which is re-written as below:

$$P_{+,g} = Pr \left(\beta \max_{i=1, \dots, p} |w_i| \geq \left| \sum_{i=1}^p w_i u_i \right| \right) \leq \int_0^\infty 2p[2\Phi(t) - 1]^{p-1} [2\Phi(\beta t / \|u\|) - 1] \phi(t) dt. \quad (24)$$

Next, we provide a simulation study to justify the approximation and compare different distributions in terms of their impact on the probability (22), for $\beta = 1$ as well as $\beta = 0.1$. For simplicity, we simulate the data as a p -dimensional vector of uniform random numbers sampled from $unif[-1, 1]$. We experiment with five different choices of w : the standard Gaussian, the uniform, the ‘‘very sparse’’ distribution (10) with $s = 1$, $s = 3$, and $s = 10$. We vary p from 10 to 1000. For each case, we repeat the simulations 10^7 times to ensure sufficient accuracy. Figure 7 verifies that the two approximations (23) and (24) are accurate. In Figure 8, we provide the curves for more types of projection matrices. From both figures, we see that using the Rademacher projection can considerably reduce (22) compared with Gaussian (and other) projections, leading to a smaller N_+ value. This typically implies better utility.

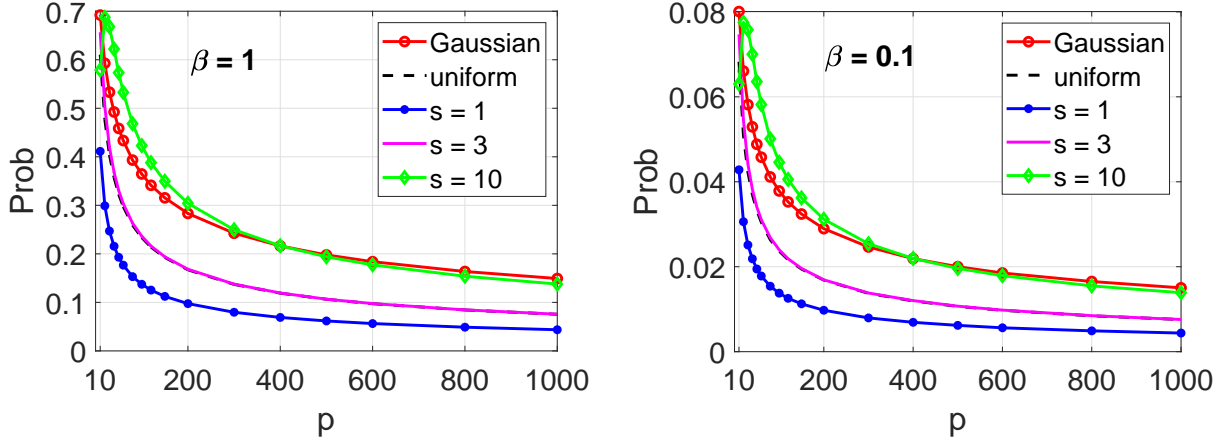


Figure 8: Simulations (same as in Figure 8) for evaluating (22), using five different choices for w : the Gaussian, the uniform, the “very sparse” distribution (10) with $s = 1, 3$ and 10. $s = 1$ is the Rademacher distribution. The data vector is simulated by sampling each entry from $unif[-1, 1]$.

L_j in DP-SignRP-RR-smooth. Similarly, we numerically evaluate the L_j in Algorithm 7. We run Algorithm 7 with $k = 512$, which gives 512 L_j values. In Figure 9, we plot the proportion (or the approximated distribution) of the values of L_j among k projections. As we see, Rademacher projection produces the least number of small L_j values and the largest number of higher L_j values. As the smooth flipping probability equals $\frac{1}{\exp(\frac{L_j}{k}\epsilon)+1}$, larger L_j leads to smaller probability of sign flipping. Hence, Rademacher is again the best choice for the projection matrix.

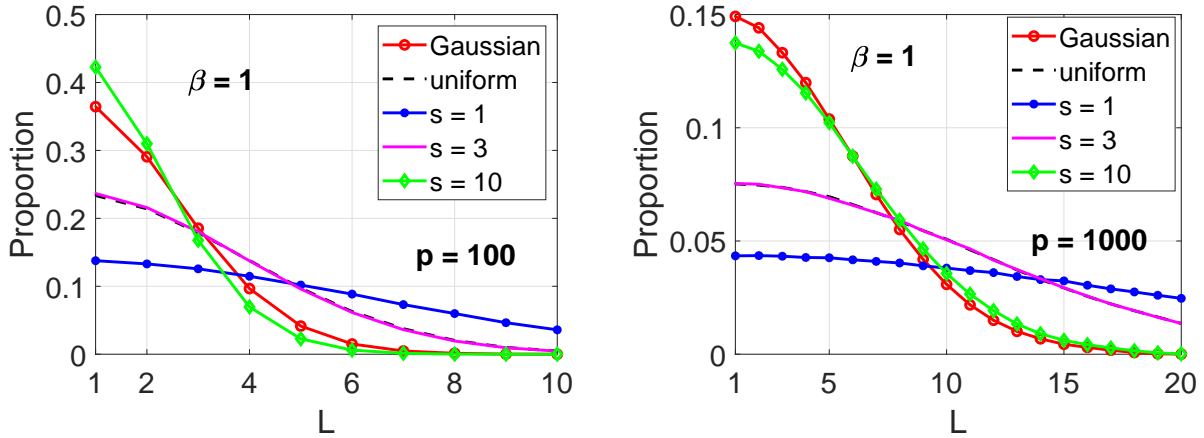


Figure 9: Simulations for evaluating L_j in Algorithm 7, using different choices for w . $s = 1$ is the Rademacher distribution. Left: $p = 100$, right: $p = 1000$. The y -axis is the proportion (normalized histogram) of the values of all the L_j , $j = 1, \dots, k$ computed using $k = 512$ projected samples.

4.4 DP-SignOPORP with Smooth Flipping Probability

Similarly, we may also take the sign of OPORP studied before, and make it differentially private. The smoothed flipping probability can also be adopted in this case. As before, we present the variant with Rademacher projection for conciseness. Algorithm 8 provides the general framework, covering two variants. The first one, DP-SignOPORP-RR, is based on the standard randomized

response (RR) technique. The second variant, DP-SignOPORP-RR-smooth, is an improved version with our proposed “smooth flipping probability”.

Algorithm 8: DP-SignOPORP-RR and DP-SignOPORP-RR-smooth

- 1 **Input:** Data $u \in [-1, 1]^p$; $\epsilon > 0$; Number of projections k
 - 2 **Output:** Differentially private sign OPORP
 - 3 Apply Algorithm 4 with a random Rademacher projection vector to get the OPORP x
 - 4 **DP-SignOPORP-RR:**
 Compute $\tilde{s}_j = \begin{cases} \text{sign}(x_j), & \text{with prob. } \frac{e^\epsilon}{e^\epsilon+1} \\ -\text{sign}(x_j), & \text{with prob. } \frac{1}{e^\epsilon+1} \end{cases}$ for $j = 1, \dots, k$
 - 5 **DP-SignOPORP-RR-smooth:**
 Compute $L_j = \lceil \frac{|x_j|}{\beta} \rceil$ for $j = 1, \dots, k$
 - 6 Compute $\tilde{s}_j = \begin{cases} \text{sign}(x_j), & \text{with prob. } \frac{e^{\epsilon'_j}}{e^{\epsilon'_j}+1} \\ -\text{sign}(x_j), & \text{with prob. } \frac{1}{e^{\epsilon'_j}+1} \end{cases}$ for $j = 1, \dots, k$, with $\epsilon'_j = L_j \epsilon$
 - 7 For $\tilde{s}_j = 0$, assign a random coin in $\{-1, 1\}$
 - 8 Return \tilde{s} as the DP-SignOPORP of u
-

Benefit of binning. In Algorithm 8, we see that the key difference compared with DP-SignRP methods is that, the $\frac{1}{N_+}$ (in Algorithm 6) or $\frac{1}{k}$ (in Algorithm 7) factor is removed from the flipping probability formulas, which is a significant advantage in terms of privacy. This improvement is a result of the binning step in OPORP. By Definition 2.3, two neighboring data u' and u differ in one coordinate. For SignRP, since each projected data is an aggregation of the whole data vector, when we switch from u to u' , (in principle) all k projections are possible to change. In contrast, in OPORP, since each data entry appears in only one bin, u' will only cause exactly one projected output to change, leaving all other bins untouched. This provides the intuition on the source of privacy gain of DP-SignOPORP.

Theorem 4.8. *Both variants in Algorithm 8 are ϵ -DP.*

Proof. The proof follows the idea of the proofs of DP-SignRP methods, but we need to additionally consider the empty bins. Denote x and x' as the OPORP from Algorithm 4 using a same random vector w , and let $s = \text{sign}(x)$, $s' = \text{sign}(x')$. Suppose u and u' differ in dimension i , and dimension i is assigned to the j^* -th bin with $j^* = \lceil \pi(i)/(p/k) \rceil$, where $\pi : [p] \mapsto [p]$ is the permutation in OPORP. For any $y \in \{-1, 1\}^k$, it is easy to see that to compute $\log \frac{Pr(\tilde{s}=y)}{Pr(\tilde{s}'=y)}$, it suffices to look at the j^* -th output sample because other probabilities cancel out. For the j^* -th sample, when $s_{j^*} \neq 0$ and $s'_{j^*} \neq 0$, by the same arguments as in the proof of Theorem 4.7, we know that $e^{-\epsilon} \leq \frac{Pr(s_{j^*}=a)}{Pr(s'_{j^*}=a)} \leq e^\epsilon$, $a \in \{-1, 1\}$, for both variants (DP-SignOPORP-RR and DP-SignOPORP-RR-smooth). When one of s_{j^*} and s'_{j^*} equals 0, it is also easy to see that (assume $s_{j^*} = 1$ and s'_{j^*} is a random coin)

$$1 \leq \frac{Pr(s_{j^*}) = 1}{Pr(s'_{j^*}) = 1} = \frac{2e^\epsilon}{e^\epsilon + 1} \leq e^\epsilon, \quad e^{-\epsilon} \leq \frac{Pr(s_{j^*}) = -1}{Pr(s'_{j^*}) = -1} = \frac{2}{e^\epsilon + 1} \leq 1.$$

This holds for both variants. In particular, this case corresponds to $L_{j^*} = 1$ for the smooth flipping probability. This proves the theorem. \square

Multiple repetitions. In Algorithm 8 Line 7, we see that if OPORP generates an empty bin (i.e., $x_j = 0$), we must assign a random sign to maintain DP. This would undermine the utility since a random coin does not provide any useful information. Therefore, it is desirable to avoid empty bins for better utility. One simple way is to repeat the DP-SignOPORP (with smaller k) for $t > 1$ times, and concatenate the output vectors. Repetition is a standard strategy for count-sketch (Charikar et al., 2004). For example, if the target $k = 256$, we may run Algorithm 8 for $t = 4$ times, each time with $256/4 = 64$ projected values and privacy budget $\epsilon/4$. Since we are using fewer bins per run, the number of empty bins will be reduced. After concatenating the 4 output vectors, we still get a 256-dimensional bit vector with ϵ -DP by the composition theorem. In the experiments, we will see that this strategy may improve the overall performance of DP-SignOPORP.

5 Experiments

We present a set of experiments on retrieval and classification tasks to demonstrate the performance of different DP-RP and DP-SignRP methods. Specifically, we will compare the following algorithms:

- Raw-data-G-OPT: the method of directly adding optimal Gaussian noise with sensitivity β to the original data vectors.
- DP-RP-G (Algorithm 1 + Theorem 3.1): Gaussian DP-RP with the Gaussian mechanism.
- DP-RP-G-OPT (Algorithm 1 + Theorem 3.5): DP-RP with Gaussian random projection matrix and the optimal Gaussian noise.
- DP-RP-G-OPT-B (Algorithm 3): DP-RP with Rademacher random projection matrix and the optimal Gaussian noise mechanism.
- DP-OPORP (Algorithm 5): OPORP algorithm with optimal Gaussian noise.
- DP-SignOPORP-RR and DP-SignOPORP-RR-smooth (Algorithm 8): Signed OPORP with standard randomized response and smooth flipping probability, respectively.

As noted in Section 4.4, due to the feature binning procedure, DP-SignOPORP is substantially better than DP-SignRP in terms of privacy protection. Therefore, we present the better-performing DP-SignOPORP method in our experiments. For conciseness, we will only present results for $\beta = 1$ and $\epsilon \in [0.1, 20]$. The chosen ϵ values cover the common range of ϵ in many DP applications (e.g., Haeberlen and Khanna (2014); Kenny et al. (2021)). Also, we fix $\delta = 10^{-6}$ for approximate (ϵ, δ) -DP algorithms.

5.1 Similarity Search

We first test the methods in similarity search problems, which is an important application of RP and SignRP in industrial applications. In this experiment, we use two standard image retrieval datasets, MNIST (LeCun et al., 1998) and CIFAR (Krizhevsky and Hinton, 2009). The MNIST dataset contains 60000 28×28 handwritten digits as the training set, and 10000 digits for testing. The CIFAR dataset includes 60000 natural images with size 32×32 (gray-scale) in total, with a 50000/10000 train-test split. On these two datasets, the pixel values are between 0 and 1 by nature. For both datasets, we treat the training set as the database, and use the samples from the test set as the queries. We set the true neighbors for each query as the top-50 sample vectors with the highest cosine similarity to the query. To search with DP-RP (and DP-OPORP), we

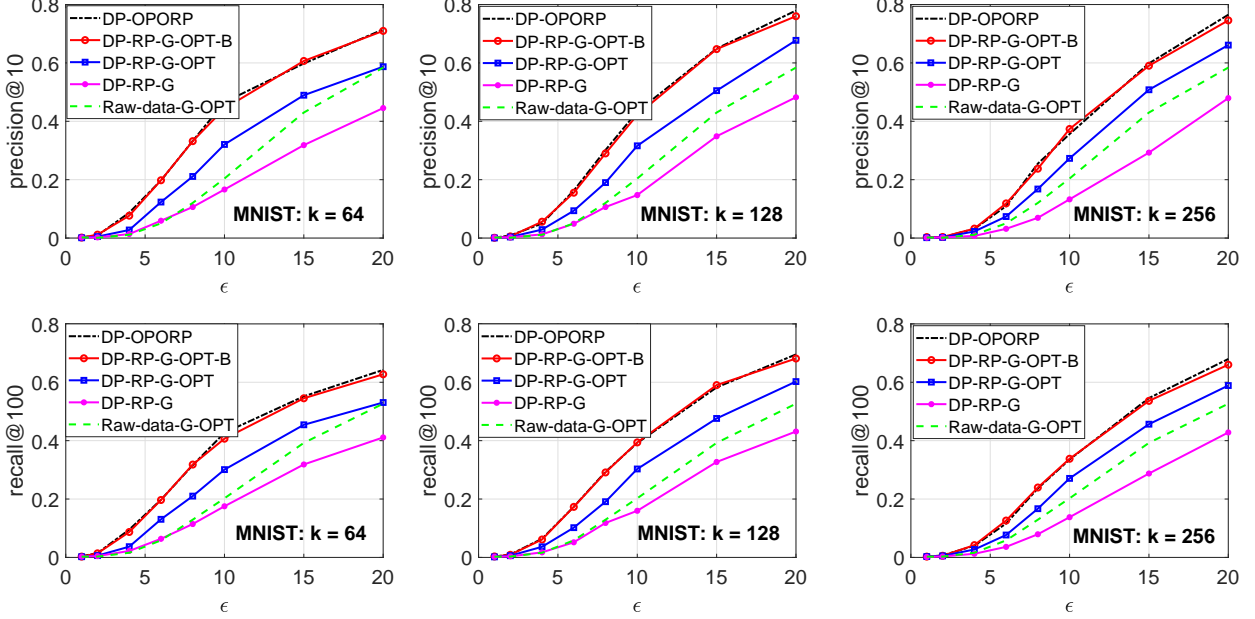


Figure 10: Retrieval recall and precision on MNIST, $\beta = 1$, $\delta = 10^{-6}$.

estimate the cosine between a query and a sample point by the cosine between their corresponding output noisy projected values. For DP-SignRP (and DP-SignOPORP), we compute the Hamming distances between the private bit vectors between the query and the database points. For both approaches, we return the samples with highest cosine or smallest Hamming distance to the query. The evaluation metrics are precision and recall, defined as

$$\text{precision@}R = \frac{\# \text{ of true positives in } R \text{ retrieved points}}{R},$$

$$\text{recall@}R = \frac{\# \text{ of true positives in } R \text{ retrieved points}}{\# \text{ of gold-standard neighbors}},$$

and in our setting, the number of gold-standard neighbors per query is 50. Our presented results are also averaged over 10 independent repetitions.

Results. In Figure 10 and Figure 11, we plot the precision and recall of DP-RP DP-OPORP algorithms on MNIST and CIFAR, respectively. In each plot, we fix a number of projections k and plot the metrics against ϵ . We observe the following:

- As a result of the optimal Gaussian mechanism, DP-RP-G-OPT substantially outperforms the prior method, DP-RP-G, in terms of search precision and recall at all ϵ . DP-RP-G-OPT-B further improves DP-RP-G-OPT considerably, demonstrating that the Rademacher projection matrix should be suggested for DP-RP.
- DP-OPORP achieves very similar utility (almost overlapping curves) with the best DP-RP variant, DP-RP-G-OPT-B, in this privacy regime. In practice, DP-OPORP might be more favorable because of its computational efficiency. These two methods provide much higher precision and recall than the Gaussian mechanism applied to the original data. On CIFAR, DP-OPORP performs slightly better than DP-RP-G-OPT-B, which may partially be explained by the extra variance reduction factor $\frac{p-k}{p-1}$ of DP-OPORP as in Theorem 3.9 and Theorem 3.10.

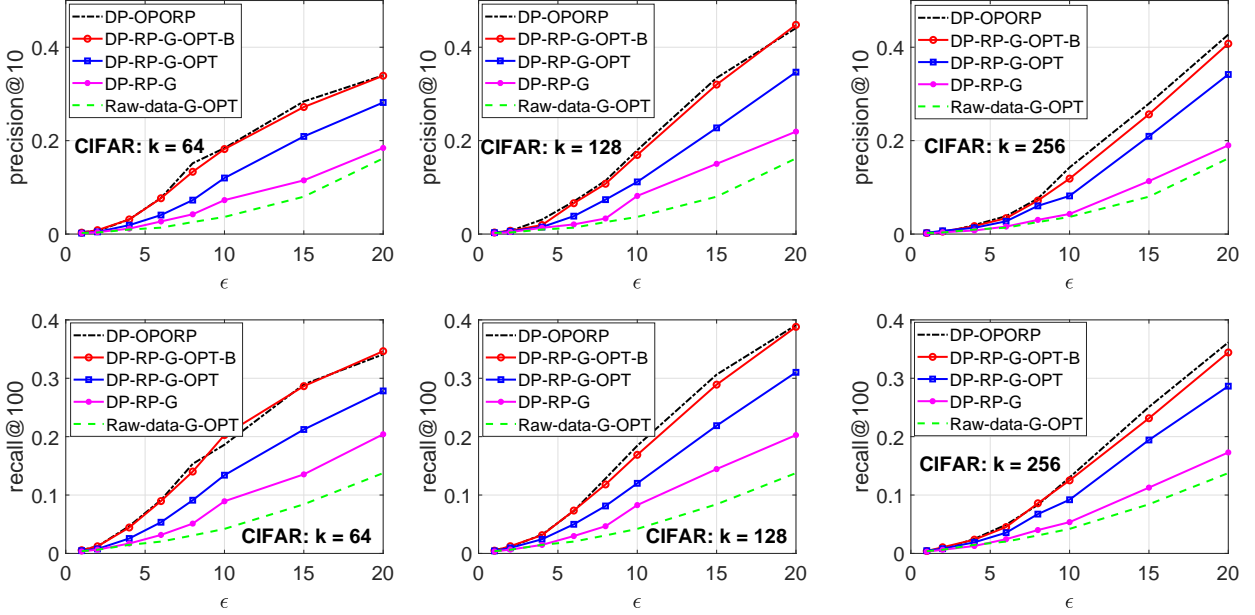


Figure 11: Retrieval recall and precision on CIFAR, $\beta = 1$, $\delta = 10^{-6}$.

5.2 SVM Classification

The RP and SignRP methods can be used to train machine learning models. We evaluate the performance of DP-SignRP-RR in classification problems trained by Support Vector Machine (SVM) (Cortes and Vapnik, 1995). We the algorithms on the WEBSpAM dataset from the LIBSVM website (Chang and Lin, 2011). We apply the “max normalization”, i.e., divide each data column by its largest magnitude such that the data entries are bounded in $[0, 1]$. As the WEBSpAM dataset was generated from 3-grams (character n -grams), the data vectors are very high-dimensional and extremely sparse. Thus, this dataset reveals a serious disadvantage of adding noise directly to the original data, because adding noise this way generates fully dense data vectors. In order to conduct the experiments, we only used 10K data samples for training and another 10K samples for testing and remove all features that are empty. By this preprocessing, the data dimensionality of the WEBSpAM dataset is reduced from the original 16 million to “merely” 250K. On the other hand, RP-type of methods (including OPORP) does not suffer from this problem because with k RP samples we obtain a dataset of only k dimensions.

We report the test accuracy for various DP methods in Figure 12. The conclusions are similar to those in the retrieval tasks: (i) DP-RP-G-OPT-B and DP-OPORP attain the highest accuracy among all full-precision RP-type algorithms, and are significantly better than Raw-data-G-OPT. This experiment again confirms the effectiveness of DP-RP and DP-OPORP for data privatization.

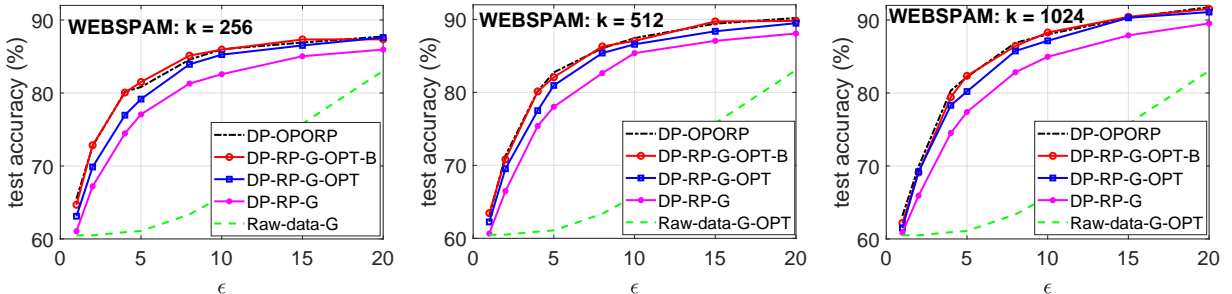


Figure 12: SVM classification on WEBSpAM, $\beta = 1$, $\delta = 10^{-6}$.

5.3 Results for DP-SignOPORP

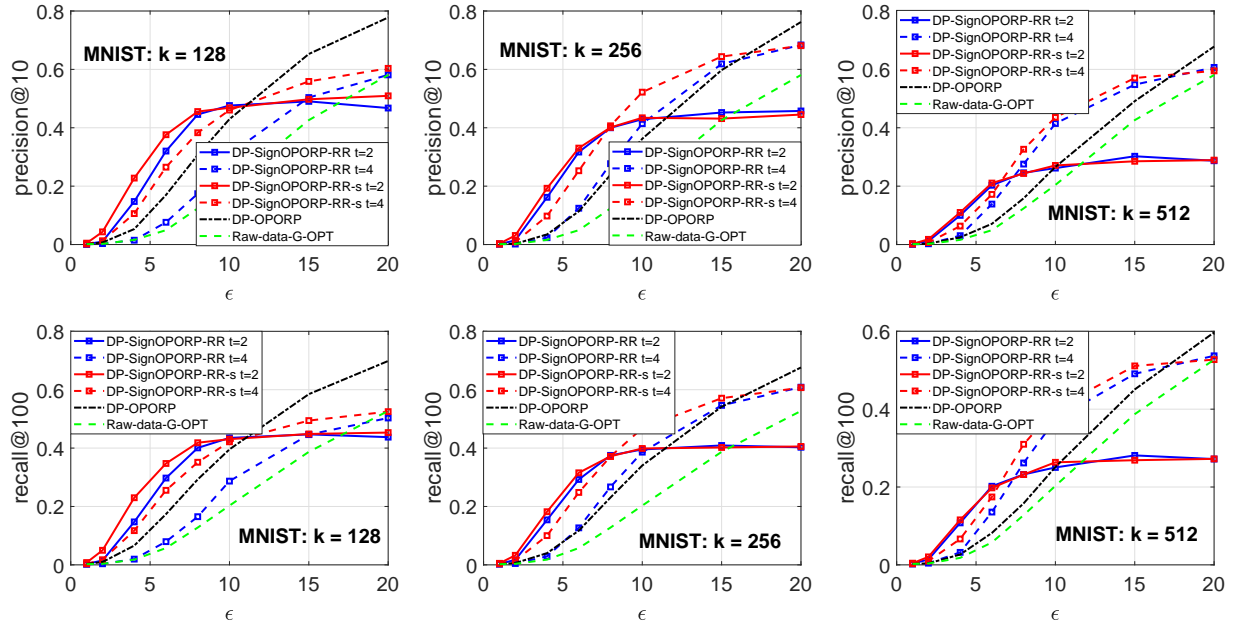


Figure 13: Retrieval on MNIST with DP-SignOPORP-RR and DP-SignOPORP-RR-smooth (in the caption, “-s” stands for “-smooth”). For DP-OPORP and Raw-data-G-OPT, we let $\delta = 10^{-6}$.

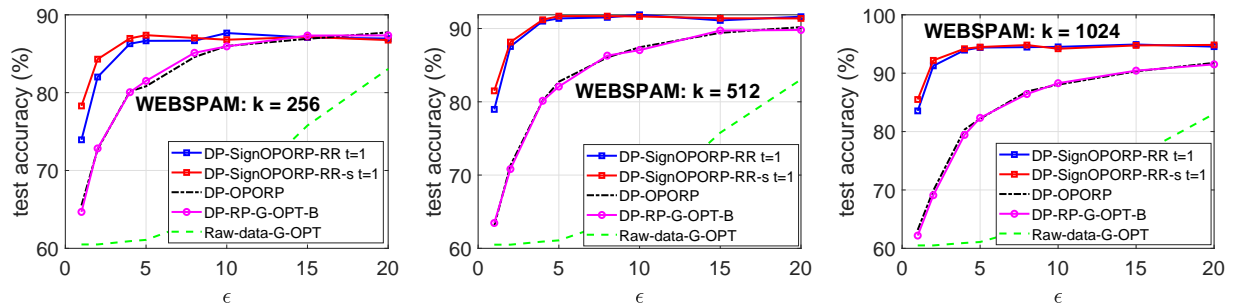


Figure 14: Classification accuracy on Webspam with DP-SignOPORP-RR and DP-SignOPORP-RR-s. For DP-OPORP and Raw-data-G-OPT, we let $\delta = 10^{-6}$.

In Figure 13, we plot the precision and recall of DP-SignOPORP-RR (with standard randomized response), and DP-SignOPORP-RR-smooth (with smooth flipping probability). In this figure, we present the results with repetition $t = 2, 4$ which yield good overall performance. As we can see, (i) the proposed smooth flipping probability considerably improves the standard randomized response technique, and (ii) DP-SignOPORP, in general, provides better search accuracy than DP-OPORP when $\epsilon < 10 \sim 15$. This range of ϵ is common in the use cases of DP for providing reasonable privacy protection. Also, we note that using a smaller t (repetitions) typically performs better when ϵ is relatively small, but worse when ϵ is large.

In Figure 14, we report the results on SVM classification. For this task, we plot DP-SignOPORP with $t = 1$. We again observe the advantage of DP-SignOPORP over DP-OPORP, and the advantage of the smooth flipping probability over the standard randomized response. Specifically, when $\epsilon \approx 5$, the test accuracy of Raw-data-G-OPT is around 60% (for WEBSHAM this is almost the same as random guessing), but DP-SignOPORP can achieve 95% accuracy with $k = 1024$.

6 iDP-SignRP Under Individual Differential Privacy (iDP)

We provide additional algorithms and evaluation on the so-called “individual differential privacy” (iDP, Definition 2.6) (Soria-Comas et al., 2017), a relaxation of standard DP which aims at improving the utility of private algorithms. iDP treats the dataset u as the “ground truth” to be protected. The “indistinguishability” requirement is only cast on u and its neighbors specifically, instead of on any possible dataset. Therefore, operationally, in the noise addition mechanisms for example, iDP essentially follows the local sensitivity (Definition 2.4) when computing the noise level, which can be much smaller than that required by the standard DP. iDP has achieved excellent utility for computing robust statistics at small ϵ (Soria-Comas et al., 2017). While iDP does not provide the same level of privacy protection as the “worst-case” standard DP, it might be sufficient in certain application scenarios, e.g., data publishing/release, when the procedure is non-interactive and the released dataset is indeed the target that one is interested in privatizing.

For the DP algorithms that have been discussed previously in this paper, we first note that, for DP-RP and DP-OPORP, the local sensitivity at any $u \in \mathcal{U}$ equals the global sensitivity. In other words, iDP does not help improve DP-RP and DP-OPORP. Also, we will soon discuss the reason why SignRP can be much better than SignOPORP under iDP. Therefore, we will mainly investigate the SignRP algorithms under iDP.

We propose two iDP-SignRP methods, based on noise addition and sign flipping, respectively. Both approaches share the same key idea of iDP, that is, many signs of the projected values do not need perturbations. This can be seen from Figure 6, where the “local flipping probability” is non-zero only in the regime when the projected data is near 0 (i.e., $L = 1$ in Algorithm 7). Since in other cases the local flip probability is zero, perturbation is not needed. As a result, out of k projections, only a fraction of the projected values needs to be perturbed. This significantly reduces the noise injected to SignRP and boosts the utility by a very large margin.

6.1 iDP-SignRP-G by Gaussian Noise Addition

In Algorithm 9, we present the iDP-SignRP-G method for one data vector u . We use the “local flipping probability” (e.g., in Figure 6) to choose which projections are perturbed before taking signs. After applying random projection to get k projected values, we do the following steps:

1. We compute noise-indicators (I_1, \dots, I_k) for each projected value in $x = \frac{1}{\sqrt{k}}W^T u$ using Algorithm 10. Denote $\mathcal{A} = \{I_j : I_j = 1, j = 1, \dots, k\}$ and $N_+ = |\mathcal{A}|$. This is the maximal number of different signs of x and $x' = W^T u', \forall u' \in Nb(u)$.
2. We compute the sensitivity $\Delta_2 = \beta \max_{i=1, \dots, p} \|W_{[i, \mathcal{A}]}\|$, where $W_{[i, \mathcal{A}]}$ denotes the i -th row of W indexed at \mathcal{A} , which is an N_+ -dimensional vector.
3. We use the optimal Gaussian mechanism (Theorem 3.5) to compute σ , with Δ_2 computed above and privacy parameters (ϵ, δ) .
4. For $j = 1, \dots, k$, if $j \notin \mathcal{A}$, we take $\tilde{s}_j = \text{sign}(x_j)$; if $j \in \mathcal{A}$, we take $\tilde{s}_j = \text{sign}(x_j + G)$ where $G \sim N(0, \sigma^2)$ is a Gaussian noise. Finally we output $\tilde{s} = [\tilde{s}_1, \dots, \tilde{s}_k]$.

Let’s explain the intuition behind DP-SignRP-G. Since a neighboring data vector u' only differs from u in one dimension by at most β , for each single projection w , when $\beta \max_{i=1, \dots, p} |w_i| \leq |w^T u|$, there is no neighbor u' of u that may change the sign of the projected value of u , i.e., $\text{sign}(w^T u') \neq$

Algorithm 9: iDP-SignRP-G (DP-SignRP with Gaussian noise)

- 1 **Input:** Data $u \in [-1, 1]^p$; Privacy parameters $\epsilon > 0$, $\delta \in (0, 1)$; Number of projections k
 - 2 **Output:** Differentially private sign random projections
 - 3 Apply RP by $x = \frac{1}{\sqrt{k}}W^T u$, where $W \in \mathbb{R}^{p \times k}$ is a random Rademacher matrix
 - 4 For every projected value in x , compute (I_1, \dots, I_k) by Algorithm 10
 - 5 Let $\mathcal{A} = \{I_j : I_j = 1, j = 1, \dots, k\}$ and $\tilde{N}_+ = |\mathcal{A}|$
 - 6 Compute sensitivity $\Delta_2 = \beta \sqrt{\frac{\tilde{N}_+}{k}}$
 - 7 Compute σ by Theorem 3.5 with Δ_2 and privacy budget ϵ and δ
 - 8 Compute $\tilde{s}_j = \begin{cases} \text{sign}(x_j), & j \notin \mathcal{A} \\ \text{sign}(x_j + G), & j \in \mathcal{A} \end{cases}$, where $G \sim N(0, \sigma^2)$ is iid Gaussian noise
 - 9 Return $\tilde{s} = [\tilde{s}_1, \dots, \tilde{s}_k]$
-

Algorithm 10: Compute noise-indicator of iDP-SignRP-G for one projection

- 1 **Input:** Data $u \in [-1, 1]^p$; one projected value z ; adjacency parameter β
 - 2 **Output:** Indicator I w.r.t. projection w for data vector u
 - 3 $I = 0$
 - 4 **If** $\beta/\sqrt{k} \geq |z|$
 - 5 $I = 1$
 - 6 **End If**
-

$\text{sign}(w^T u)$. In other words, when $\beta \max_{i=1, \dots, p} |w_i| \leq |w^T u|$, no noise is needed for this projected value to attain iDP. This is the reason why we call the output of Algorithm 10 a “noise-indicator”. Consequently, in step 4 of iDP-SignRP-G it suffices to add Gaussian noise only to those projected values x_j with $j \in \mathcal{A}$, instead of to all k projections as in DP-RP-G-OPT.

Theorem 6.1 (iDP-SignRP-G). *Algorithm 9 is (ϵ, δ) -iDP for data u .*

Proof. For a data vector u , let $Nb(u)$ be its neighbor set with vectors that differ from u by at most β in one dimension. Denote $x = \frac{1}{\sqrt{k}}W^T u$ and $x' = \frac{1}{\sqrt{k}}W^T u'$. Let (I_1, \dots, I_k) be the noise-indicators from Algorithm 10 and $\mathcal{A} = \{i : I_i = 1\}$, $\tilde{N}_+ = |\mathcal{A}|$. Consider the two sets separately:

- For $j \in [k] \setminus \mathcal{A}$, by the condition $\beta/\sqrt{k} \leq |z|$, we know that $\forall u' \in Nb(u)$, it holds that $\text{sign}(x_j) = \text{sign}(x'_j)$.
- For $j \in \mathcal{A}$, consider the sub-vector $x_{\mathcal{A}}$. Adding iid Gaussian noise to $x_{\mathcal{A}}$ according to Theorem 3.5 with $\Delta_2 = \beta \sqrt{\frac{\tilde{N}_+}{k}}$ ensures the (ϵ, δ) -DP of $x_{\mathcal{A}}$. By the post-processing property of DP, we know that $\text{sign}(x_{\mathcal{A}})$ is also (ϵ, δ) -DP. Thus, for any $Q \in \{-1, 1\}^{N_+}$, we have $\Pr(\text{sign}(x_{\mathcal{A}}) = Q) - e^\epsilon \Pr(\text{sign}(x'_{\mathcal{A}}) = Q) \leq \delta$, $\forall u' \in Nb(u)$.

Combining two parts, we have for any $Q \in \{-1, 1\}^k$,

$$\Pr(\text{sign}(x) = Q) - e^\epsilon \Pr(\text{sign}(x') = Q) = \Pr(\text{sign}(x_{\mathcal{A}}) = Q) - e^\epsilon \Pr(\text{sign}(x'_{\mathcal{A}}) = Q) \leq \delta,$$

for all $u' \in Nb(u)$. By the symmetry of DP (on the sub-vector $x_{\mathcal{A}}$), we also know that $\Pr(\text{sign}(x') = Q) - e^\epsilon \Pr(\text{sign}(x) = Q) \leq \delta$. This proves the (ϵ, δ) -iDP by Definition 2.6. \square

6.2 iDP-SignRP-RR by Randomized Response

Algorithm 11: iDP-SignRP-RR

- 1 **Input:** Data $u \in [-1, 1]^p$, privacy parameters $\epsilon > 0$, $0 < \delta < 1$, number of projections k
 - 2 **Output:** Differentially private sign random projections
 - 3 Apply RP by $x = \frac{1}{\sqrt{k}}W^T u$, where $W \in \mathbb{R}^{p \times k}$ is a random Rademacher matrix
 - 4 For every column in W , compute (I_1, \dots, I_k) by Algorithm 10
 - 5 Let $\mathcal{A} = \{I_j : I_j = 1, j = 1, \dots, k\}$ and $\tilde{N}_+ = |\mathcal{A}|$
 - 6 Compute $\tilde{s}_j = \begin{cases} \text{sign}(x_j), & j \notin \mathcal{A} \\ \text{sign}(x_j), & j \in \mathcal{A} \text{ with prob. } \frac{e^{\epsilon'}}{e^{\epsilon'}+1} \\ -\text{sign}(x_j), & j \in \mathcal{A} \text{ with prob. } \frac{1}{e^{\epsilon'}+1} \end{cases}$ for $j = 1, \dots, k$, with $\epsilon' = \epsilon/\tilde{N}_+$
 - 7 Return \tilde{s} as the DP-SignRP of u
-

Similar to Section 4, we also have an iDP-SignRP-RR method with pure ϵ -DP by random sign flipping, as summarized in Algorithm 11. After we apply random projection $x = \frac{1}{\sqrt{k}}W^T u$, we call the same procedure as in iDP-SignRP-G to determine set \mathcal{A} representing the projected values that need perturbation for iDP. For $j \notin \mathcal{A}$, we use the original $\tilde{s}_j = \text{sign}(x_j)$. For $j \in \mathcal{A}$, we keep $\text{sign}(x_j)$ with probability $\frac{e^{\epsilon'}}{e^{\epsilon'}+1}$ and flip the sign otherwise, where $e^{\epsilon'} = \epsilon/\tilde{N}_+$ with $\tilde{N}_+ = |\mathcal{A}|$.

Theorem 6.2. *Algorithm 11 achieves ϵ -iDP for data u .*

Proof. The high-level proof idea is similar to that of Theorem 6.1. For $u \in [-1, 1]^p$ let u' be an β -neighboring data. Let $s = \text{sign}(W^T u) \in \{-1, +1\}^k$, $s' = \text{sign}(W^T u') \in \{-1, +1\}^k$, and denote \tilde{s} and \tilde{s}' as the randomized output of s and s' by Algorithm 11, respectively. Consider \mathcal{A} in Algorithm 11. By Algorithm 10, we know that for $j \notin \mathcal{A}$, $\Pr(\tilde{s}_j = \tilde{s}'_j) = \Pr(s_j = s'_j) = 1$, $\forall u' \in \text{Nb}(u)$. For projections in \mathcal{A} , denote $S = \{j \in \mathcal{A} : s_j \neq s'_j\}$ and $S^c = \mathcal{A} \setminus S$. For any vector $y \in \{-1, +1\}^k$, we further define $S_0 = \{j \in S : s_j = y_j\}$, $S_1 = \{j \in S : s_j \neq y_j\}$, $S_0^c = \{j \in S^c : s_j = y_j\}$ and $S_1^c = \{j \in S^c : s_j \neq y_j\}$. Since the k projections are independent, by composition we have

$$\begin{aligned} \log \frac{\Pr(\tilde{s} = y)}{\Pr(\tilde{s}' = y)} &= \log \frac{\prod_{j \notin \mathcal{A}} \Pr(\tilde{s}_j = y_j) \prod_{j \in S_0^c} \frac{e^{\epsilon'}}{e^{\epsilon'}+1} \prod_{j \in S_1^c} \frac{1}{e^{\epsilon'}+1} \prod_{j \in S_0} \frac{e^{\epsilon'}}{e^{\epsilon'}+1} \prod_{j \in S_1} \frac{1}{e^{\epsilon'}+1}}{\prod_{j \notin \mathcal{A}} \Pr(\tilde{s}'_j = y_j) \prod_{j \in S_0^c} \frac{e^{\epsilon'}}{e^{\epsilon'}+1} \prod_{j \in S_1^c} \frac{1}{e^{\epsilon'}+1} \prod_{j \in S_0} \frac{1}{e^{\epsilon'}+1} \prod_{j \in S_1} \frac{e^{\epsilon'}}{e^{\epsilon'}+1}} \\ &\leq \log \frac{\prod_{j \in S} \frac{e^{\epsilon'}}{e^{\epsilon'}+1}}{\prod_{j \in S} \frac{1}{e^{\epsilon'}+1}} = |S|\epsilon' \leq \tilde{N}_+\epsilon' = \epsilon, \end{aligned}$$

which proves the ϵ -iDP according to Definition 2.6. \square

The number of projections that requires noise addition, \tilde{N}_+ , is also tightly related to the $P_+(\|u\|, p)$ (Proposition 4.5 and (18)). Particularly, \tilde{N}_+ would be small when the data has a relatively large norm compared with the change in neighboring data β . Therefore, both iDP-SignRP methods would have better utility when the data norm is large. The reduction from k to \tilde{N}_+ also leads to smaller Gaussian noise or smaller flipping probability for the values that need to be perturbed. Specifically, note that in Algorithm 9, the optimal Gaussian mechanism is deployed with sensitivity $\Delta_2 = \beta\sqrt{\frac{\tilde{N}_+}{k}}$, instead of $\Delta_2 = \beta$ as in (8) for DP-RP-G-OPT.

iDP-SignOPORP. Similarly, we can also apply iDP to the SignOPORP method. Basically, we only need to replace x in Line 3 in both Algorithm 9 and Algorithm 11 by the OPORP of u . However, we note that this iDP-SignOPORP procedure is considerably worse than iDP-SignRP in performance. This is because, by the binning step in OPORP, the average scale of each projected value becomes much smaller. This implies that in Algorithm 10, the magnitude of z would be much smaller, so a lot more projected values will require perturbation, which leads to a utility loss. This illustrates the superiority of SignRP under iDP: since each RP aggregates the whole data vector, SignRP is more robust to a small change in the data. Hence, less noise is needed.

6.3 Empirical Results on iDP

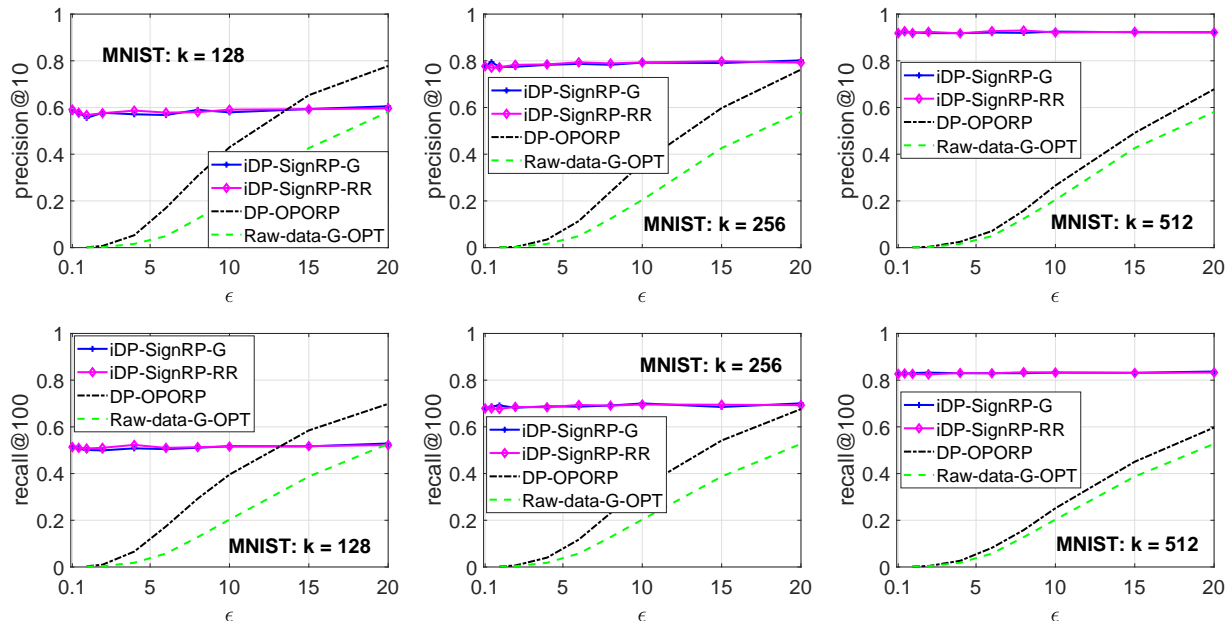


Figure 15: Retrieval on MNIST with iDP-SignRP, $\beta = 1$, $\delta = 10^{-6}$.

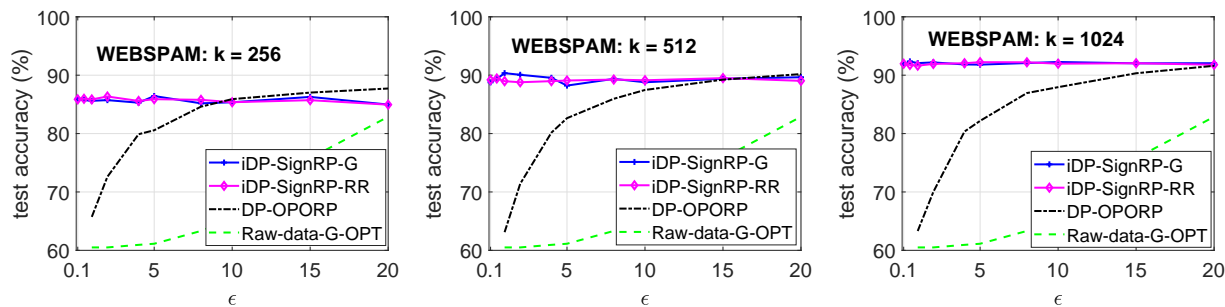


Figure 16: SVM on WEBSpAM with iDP-SignRP, $\beta = 1$, $\delta = 10^{-6}$.

To demonstrate the empirical gain in utility of iDP-SignRP, we conduct the same set of experiments as in Section 5. Figure 15 reports the precision and recall on MNIST, and Figure 16 presents the SVM test accuracy on WEBSpAM. As we can see, iDP-SignRP achieves very high utility even when $\epsilon < 0.1$. We see that the curves of iDP-SignRP are almost flat. This is because only a small fraction of projected values are perturbed, so the untouched projected values already provide rich information for search and classification. In other words, the experimental results illustrate that the SignRP itself is already very strong in protecting the individual differential privacy. In other

words, SignRP itself is already a strong method to protect the privacy of each specific dataset with respect to the individual DP, e.g., in non-interactive data publishing tasks.

7 Conclusion

The concept of differential privacy (DP) has been widely accepted as an elegant mathematical framework for protecting data privacy. In practice, however, deploying DP algorithms often leads to considerably worse performance (utility). For example, if we directly add noise to high-dimensional data vectors, the required noise level (i.e., the variance of the noise random variables) is often quite high which can severely degrade the performance of the subsequent tasks. Furthermore, inserting noise to the original data completely destroys data sparsity. For example, in text data or data for commercial advertising CTR models, for each data vector, typically only a very small fraction of the coordinates are non-zero. Adding noise to the original dataset can easily generate dense vectors in millions or even billions dimensions. Therefore, DP algorithms based on random projections (RP), which is an effective tool for dimension reduction, can be desirable. This is our motivation.

Our key contribution is the observation that the signs of the randomly projected data vectors can be very stable when the original data vectors are perturbed. That is, we let $x = \sum_{i=1}^p u_i w_i$, where u is the original p -dimensional data vector and w is a projection vector. The sign $sign(x) = sign(\sum_{i=1}^p u_i w_i)$ can be changed if u is modified to be u' , with a probability which depends on the choice of the distribution of w . Our study reveals that such (sign-flipping) probability can be quite low (e.g., < 0.1), under the common definition of “neighbors” in DP. This is the basis for our work.

In this study, we have developed two lines of strategies for taking advantage of this sign-flipping probability. By leveraging the idea of smooth sensitivity, we propose a “smooth flipping” strategy which satisfies the rigorous definition of DP. The algorithm we recommend is named **DP-SignOPORP** by using a variant of the count-sketch for generating the projection vectors. In a recent work, [Li and Li \(2023a\)](#) proposed “one-permutation + one random projection” (OPORP) which improves the original count-sketch in two aspects: (i) fixed-length binning, and (ii) normalization. In this study, we have observed that DP-SignOPORP noticeably outperforms other DP-RP algorithms.

We have also exploited the other direction for utilizing the sign-flipping probability of random projections, by leveraging the concept of “individual differential privacy” (iDP) and “local sensitivity”. The proposed “iDP-SignRP” algorithms perform remarkably well, in that they are able to achieve excellent utility even at very small ϵ values (e.g., $\epsilon < 0.5$). Although iDP does not strictly satisfy DP, it is anticipated that iDP might be still useful for certain applications such as releasing datasets.

The family of DP-RP and DP-SignRP algorithms can be conveniently used in training AI models for protecting the privacy of input features. A notable use case would be the embedding-based retrieval (EBR), which is nowadays widely adopted in commercial applications. Embeddings are trained/stored and then might be shared across different countries/companies/business units. For example, it is common that embeddings trained from one model might be used as the input feature data for other models. Understandably, privacy alarms might be triggered in those applications.

Acknowledgement

The authors would like to thank colleagues from Microsoft Research: Janardhan Kulkarni, Yin Tat Lee, Sergey Yekhanin, for helpful discussions.

References

- Martín Abadi, Andy Chu, Ian J. Goodfellow, H. Brendan McMahan, Ilya Mironov, Kunal Talwar, and Li Zhang. Deep learning with differential privacy. In *Proceedings of the 2016 ACM SIGSAC Conference on Computer and Communications Security (CCS)*, pages 308–318, Vienna, Austria, 2016.
- Dimitris Achlioptas. Database-friendly random projections: Johnson-lindenstrauss with binary coins. *J. Comput. Syst. Sci.*, 66(4):671–687, 2003.
- Naman Agarwal, Ananda Theertha Suresh, Felix X. Yu, Sanjiv Kumar, and Brendan McMahan. cpSGD: Communication-efficient and differentially-private distributed SGD. In *Advances in Neural Information Processing Systems (NeurIPS)*, pages 7575–7586, Montréal, Canada, 2018.
- Eman Abdullah AlOmar, Wajdi Aljedaani, Murtaza Tamjeed, Mohamed Wiem Mkaouer, and Yasmine N. El-Glaly. Finding the needle in a haystack: On the automatic identification of accessibility user reviews. In *Proceedings of the Conference on Human Factors in Computing Systems (CHI)*, pages 387:1–387:15, Virtual Event / Yokohama, Japan, 2021.
- Borja Balle and Yu-Xiang Wang. Improving the gaussian mechanism for differential privacy: Analytical calibration and optimal denoising. In *Proceedings of the 35th International Conference on Machine Learning (ICML)*, pages 403–412, Stockholm, Sweden, 2018.
- Ghazaleh Beigi, Ahmadreza Mosallanezhad, Ruocheng Guo, Hamidreza Alvari, Alexander Nou, and Huan Liu. Privacy-aware recommendation with private-attribute protection using adversarial learning. In *Proceedings of the Thirteenth ACM International Conference on Web Search and Data Mining (WSDM)*, pages 34–42, Houston, TX, USA, 2020.
- Arnaud Berlioz, Arik Friedman, Mohamed Ali Kâafar, Roksana Boreli, and Shlomo Berkovsky. Applying differential privacy to matrix factorization. In *Proceedings of the 9th ACM Conference on Recommender Systems (RecSys)*, pages 107–114, Vienna, Austria, 2015.
- Ella Bingham and Heikki Mannila. Random projection in dimensionality reduction: Applications to image and text data. In *Proceedings of the Seventh ACM SIGKDD International Conference on Knowledge Discovery and Data Mining (KDD)*, pages 245–250, San Francisco, CA, 2001.
- Jeremiah Blocki, Avrim Blum, Anupam Datta, and Or Sheffet. The johnson-lindenstrauss transform itself preserves differential privacy. In *Proceedings of the 53rd Annual IEEE Symposium on Foundations of Computer Science (FOCS)*, pages 410–419, New Brunswick, NJ, 2012.
- Avrim Blum, Cynthia Dwork, Frank McSherry, and Kobbi Nissim. Practical privacy: the SuLQ framework. In *Proceedings of the Twenty-fourth ACM SIGACT-SIGMOD-SIGART Symposium on Principles of Database Systems (PODS)*, pages 128–138, Baltimore, MD, 2005.
- Petros Boufounos and Richard G. Baraniuk. 1-bit compressive sensing. In *Proceedings of the 42nd Annual Conference on Information Sciences and Systems (CISS)*, pages 16–21, Princeton, NJ, 2008.
- Emmanuel J. Candès, Justin K. Romberg, and Terence Tao. Robust uncertainty principles: exact signal reconstruction from highly incomplete frequency information. *IEEE Trans. Inf. Theory*, 52(2):489–509, 2006.

- Chih-Chung Chang and Chih-Jen Lin. Libsvm: a library for support vector machines. *ACM Transactions on Intelligent Systems and Technology (TIST)*, 2(3):27, 2011.
- Moses Charikar, Kevin Chen, and Martin Farach-Colton. Finding frequent items in data streams. *Theor. Comput. Sci.*, 312(1):3–15, 2004.
- Moses S Charikar. Similarity estimation techniques from rounding algorithms. In *Proceedings of the Thiry-Fourth Annual ACM Symposium on Theory of Computing (STOC)*, pages 380–388, Montreal, Canada, 2002.
- Kamalika Chaudhuri and Claire Monteleoni. Privacy-preserving logistic regression. In *Advances in Neural Information Processing Systems (NIPS)*, pages 289–296, Vancouver, Canada, 2008.
- Kamalika Chaudhuri, Claire Monteleoni, and Anand D. Sarwate. Differentially private empirical risk minimization. *J. Mach. Learn. Res.*, 12:1069–1109, 2011.
- Danqi Chen, Adam Fisch, Jason Weston, and Antoine Bordes. Reading wikipedia to answer open-domain questions. In *Proceedings of the 55th Annual Meeting of the Association for Computational Linguistics (ACL)*, pages 1870–1879, Vancouver, Canada, 2017.
- Wenlin Chen, James Wilson, Stephen Tyree, Kilian Weinberger, and Yixin Chen. Compressing Neural Networks with the Hashing Trick. In *Proceedings of the 32nd International Conference on Machine Learning (ICML)*, pages 2285–2294, Lille, France, 2015.
- Graham Cormode, Somesh Jha, Tejas Kulkarni, Ninghui Li, Divesh Srivastava, and Tianhao Wang. Privacy at scale: Local differential privacy in practice. In *Proceedings of the 2018 International Conference on Management of Data (SIGMOD)*, pages 1655–1658, Houston, TX, 2018a.
- Graham Cormode, Tejas Kulkarni, and Divesh Srivastava. Marginal release under local differential privacy. In *Proceedings of the 2018 International Conference on Management of Data (SIGMOD)*, pages 131–146, Houston, TX, 2018b.
- Corinna Cortes and Vladimir Vapnik. Support-vector networks. *Mach. Learn.*, 20(3):273–297, 1995.
- George E. Dahl, Jack W. Stokes, Li Deng, and Dong Yu. Large-scale malware classification using random projections and neural networks. In *Proceedings of the IEEE International Conference on Acoustics, Speech and Signal Processing (ICASSP)*, pages 3422–3426, Vancouver, Canada, 2013.
- Sanjoy Dasgupta. Experiments with random projection. In *Proceedings of the 16th Conference in Uncertainty in Artificial Intelligence (UAI)*, pages 143–151, Stanford, CA, 2000.
- Sanjoy Dasgupta and Yoav Freund. Random projection trees and low dimensional manifolds. In *Proceedings of the 40th Annual ACM Symposium on Theory of Computing (STOC)*, pages 537–546, Victoria, Canada, 2008.
- Mayur Datar, Nicole Immorlica, Piotr Indyk, and Vahab S Mirrokni. Locality-sensitive hashing scheme based on p-stable distributions. In *Proceedings of the Twentieth Annual Symposium on Computational Geometry (SCG)*, pages 253–262, Brooklyn, NY, 2004.
- Damien Desfontaines and Balázs Pejő. Sok: Differential privacies. *Proc. Priv. Enhancing Technol.*, 2020(2):288–313, 2020.

- Charlie Dickens, Justin Thaler, and Daniel Ting. Order-invariant cardinality estimators are differentially private. In *Advances in Neural Information Processing Systems (NeurIPS)*, New Orleans, LA, 2022.
- Bolin Ding, Janardhan Kulkarni, and Sergey Yekhanin. Collecting telemetry data privately. In *Advances in Neural Information Processing Systems (NIPS)*, pages 3571–3580, Long Beach, CA, 2017.
- Jinshuo Dong, Aaron Roth, and Weijie J Su. Gaussian differential privacy. *Journal of the Royal Statistical Society Series B: Statistical Methodology*, 84(1):3–37, 2022.
- Wei Dong, Moses Charikar, and Kai Li. Asymmetric distance estimation with sketches for similarity search in high-dimensional spaces. In *Proceedings of the 31st Annual International ACM SIGIR Conference on Research and Development in Information Retrieval (SIGIR)*, pages 123–130, 2008.
- David L. Donoho. Compressed sensing. *IEEE Trans. Inf. Theory*, 52(4):1289–1306, 2006.
- Cynthia Dwork and Jing Lei. Differential privacy and robust statistics. In *Proceedings of the 41st Annual ACM Symposium on Theory of Computing (STOC)*, pages 371–380, Bethesda, MD, 2009.
- Cynthia Dwork and Aaron Roth. The algorithmic foundations of differential privacy. *Found. Trends Theor. Comput. Sci.*, 9(3-4):211–407, 2014.
- Cynthia Dwork and Guy N Rothblum. Concentrated differential privacy. *arXiv preprint arXiv:1603.01887*, 2016.
- Cynthia Dwork, Frank McSherry, Kobbi Nissim, and Adam D. Smith. Calibrating noise to sensitivity in private data analysis. In *Proceedings of the Third Theory of Cryptography Conference (TCC)*, pages 265–284, New York, NY, 2006.
- Úlfar Erlingsson, Vasyl Pihur, and Aleksandra Korolova. RAPPOR: randomized aggregatable privacy-preserving ordinal response. In *Proceedings of the 2014 ACM SIGSAC Conference on Computer and Communications Security (CCS)*, pages 1054–1067, Scottsdale, AZ, 2014.
- Chenglin Fan and Ping Li. Distances release with differential privacy in tree and grid graph. In *IEEE International Symposium on Information Theory (ISIT)*, pages 2190–2195, 2022.
- Chenglin Fan, Ping Li, and Xiaoyun Li. Private graph all-pairwise-shortest-path distance release with improved error rate. In *Advances in Neural Information Processing Systems (NeurIPS)*, New Orleans, LA, 2022.
- Huang Fang, Xiaoyun Li, Chenglin Fan, and Ping Li. Improved convergence of differential private sgd with gradient clipping. In *Proceedings of the Eleventh International Conference on Learning Representations (ICLR)*, Kigali, Rwanda, 2023.
- Dan Feldman, Amos Fiat, Haim Kaplan, and Kobbi Nissim. Private coresets. In *Proceedings of the 41st Annual ACM Symposium on Theory of Computing (STOC)*, pages 361–370, Bethesda, MD, 2009.
- Xiaoli Zhang Fern and Carla E. Brodley. Random projection for high dimensional data clustering: A cluster ensemble approach. In *Proceedings of the Twentieth International Conference (ICML)*, pages 186–193, Washington, DC, 2003.

- Yoav Freund, Sanjoy Dasgupta, Mayank Kabra, and Nakul Verma. Learning the structure of manifolds using random projections. In *Advances in Neural Information Processing Systems (NIPS)*, pages 473–480, Vancouver, Canada, 2007.
- Jerome H. Friedman, F. Baskett, and L. Shustek. An algorithm for finding nearest neighbors. *IEEE Transactions on Computers*, 24:1000–1006, 1975.
- Jason Ge, Zhaoran Wang, Mengdi Wang, and Han Liu. Minimax-optimal privacy-preserving sparse PCA in distributed systems. In *Proceedings of the International Conference on Artificial Intelligence and Statistics (AISTATS)*, pages 1589–1598, Playa Blanca, Lanzarote, Canary Islands, Spain, 2018.
- Michel X. Goemans and David P. Williamson. Improved approximation algorithms for maximum cut and satisfiability problems using semidefinite programming. *J. ACM*, 42(6):1115–1145, 1995.
- Anupam Gupta, Katrina Ligett, Frank McSherry, Aaron Roth, and Kunal Talwar. Differentially private combinatorial optimization. In *Proceedings of the Twenty-First Annual ACM-SIAM Symposium on Discrete Algorithms (SODA)*, pages 1106–1125, Austin, TX, 2010.
- Farzin Haddadpour, Belhal Karimi, Ping Li, and Xiaoyun Li. Fedsketch: Communication-efficient and private federated learning via sketching. *arXiv preprint arXiv:2008.04975*, 2020.
- Justin Hsu Marco Gaboardi Andreas Haeberlen and Sanjeev Khanna. Differential privacy: An economic method for choosing epsilon. *arXiv preprint arXiv:1402.3329*, 2014.
- Piotr Indyk and Rajeev Motwani. Approximate nearest neighbors: Towards removing the curse of dimensionality. In *Proceedings of the Thirtieth Annual ACM Symposium on the Theory of Computing (STOC)*, pages 604–613, Dallas, TX, 1998.
- Prateek Jain, Om Dipakbhai Thakkar, and Abhradeep Thakurta. Differentially private matrix completion revisited. In *Proceedings of the 35th International Conference on Machine Learning (ICML)*, pages 2220–2229, Stockholmsmässan, Stockholm, Sweden, 2018.
- Bargav Jayaraman and David Evans. Evaluating differentially private machine learning in practice. In *Proceedings of the 28th USENIX Security Symposium (USENIX Security)*, pages 1895–1912, Santa Clara, CA, 2019.
- William B. Johnson and Joram Lindenstrauss. Extensions of Lipschitz mapping into Hilbert space. *Contemporary Mathematics*, 26:189–206, 1984.
- Peter Kairouz, Sewoong Oh, and Pramod Viswanath. Extremal mechanisms for local differential privacy. In *Advances in Neural Information Processing Systems (NeurIPS)*, pages 2879–2887, Montreal, Canada, 2014.
- Shiva Prasad Kasiviswanathan, Kobbi Nissim, Sofya Raskhodnikova, and Adam D. Smith. Analyzing graphs with node differential privacy. In *Proceedings of the 10th Theory of Cryptography Conference (TCC)*, pages 457–476, Tokyo, Japan, 2013.
- Christopher T Kenny, Shiro Kuriwaki, Cory McCartan, Evan TR Rosenman, Tyler Simko, and Kosuke Imai. The use of differential privacy for census data and its impact on redistricting: The case of the 2020 us census. *Science advances*, 7(41):eabk3283, 2021.

- Krishnaram Kenthapadi, Aleksandra Korolova, Ilya Mironov, and Nina Mishra. Privacy via the johnson-lindenstrauss transform. *J. Priv. Confidentiality*, 5(1), 2013.
- Karin Knudson, Rayan Saab, and Rachel Ward. One-bit compressive sensing with norm estimation. *IEEE Trans. Inf. Theory*, 62(5):2748–2758, 2016.
- Alex Krizhevsky and Geoffrey Hinton. Learning multiple layers of features from tiny images. *Technical Report, University of Toronto*, 2009.
- Béatrice Laurent and Pascal Massart. Adaptive estimation of a quadratic functional by model selection. *The Annals of Statistics*, pages 1302–1338, 2000.
- Yann LeCun, Léon Bottou, Yoshua Bengio, and Patrick Haffner. Gradient-based learning applied to document recognition. *Proc. IEEE*, 86(11):2278–2324, 1998.
- Cong Leng, Jian Cheng, and Hanqing Lu. Random subspace for binary codes learning in large scale image retrieval. In *Proceedings of the 37th International ACM SIGIR Conference on Research and Development in Information Retrieval (SIGIR)*, pages 1031–1034, Gold Coast, Australia, 2014.
- Ping Li. Sign-full random projections. In *Proceedings of the Thirty-Third AAAI Conference on Artificial Intelligence (AAAI)*, pages 4205–4212, Honolulu, HI, 2019.
- Ping Li and Xiaoyun Li. OPORP: One permutation + one random projection. *arXiv preprint arXiv:2302.03505*, 2023a.
- Ping Li and Weijie Zhao. GCWSNet: Generalized consistent weighted sampling for scalable and accurate training of neural networks. In *Proceedings of the 31st ACM International Conference on Information and Knowledge Management (CIKM)*, Atlanta, GA, 2022.
- Ping Li, Trevor J Hastie, and Kenneth W Church. Very sparse random projections. In *Proceedings of the 12th ACM SIGKDD international conference on Knowledge discovery and data mining (KDD)*, pages 287–296, Philadelphia, PA, 2006.
- Ping Li, Michael Mitzenmacher, and Anshumali Shrivastava. Coding for random projections. In *Proceedings of the 31th International Conference on Machine Learning (ICML)*, pages 676–684, Beijing, China, 2014.
- Xiaoyun Li and Ping Li. Generalization error analysis of quantized compressive learning. In *Advances in Neural Information Processing Systems (NeurIPS)*, pages 15124–15134, Vancouver, Canada, 2019a.
- Xiaoyun Li and Ping Li. Random projections with asymmetric quantization. In *Advances in Neural Information Processing Systems (NeurIPS)*, pages 10857–10866, Vancouver, Canada, 2019b.
- Xiaoyun Li and Ping Li. Quantization algorithms for random Fourier features. In *Proceedings of the 38th International Conference on Machine Learning (ICML)*, pages 6369–6380, Virtual Event, 2021.
- Xiaoyun Li and Ping Li. Differentially private one permutation hashing and bin-wise consistent weighted sampling. *arXiv preprint*, 2023b.
- Ilya Mironov. Rényi differential privacy. In *Proceedings of the 30th IEEE Computer Security Foundations Symposium (CSF)*, pages 263–275, Santa Barbara, CA, 2017.

- Kobbi Nissim, Sofya Raskhodnikova, and Adam D. Smith. Smooth sensitivity and sampling in private data analysis. In *Proceedings of the 39th Annual ACM Symposium on Theory of Computing (STOC)*, pages 75–84, San Diego, CA, 2007.
- Donald Bruce Owen. A table of normal integrals: A table. *Communications in Statistics-Simulation and Computation*, 9(4):389–419, 1980.
- Stephan Rabanser, Stephan Günnemann, and Zachary C. Lipton. Failing loudly: An empirical study of methods for detecting dataset shift. In *Advances in Neural Information Processing Systems (NeurIPS)*, pages 1394–1406, Vancouver, Canada, 2019.
- Daniel Rothchild, Ashwinee Panda, Enayat Ullah, Nikita Ivkin, Ion Stoica, Vladimir Braverman, Joseph Gonzalez, and Raman Arora. FetchSGD: Communication-efficient federated learning with sketching. In *Proceedings of the 37th International Conference on Machine Learning (ICML)*, pages 8253–8265, Virtual Event, 2020.
- Anshumali Shrivastava and Ping Li. In defense of minhash over simhash. In *Proceedings of the Seventeenth International Conference on Artificial Intelligence and Statistics (AISTATS)*, pages 886–894, Reykjavik, Iceland, 2014.
- Karan Singhal, Hakim Sidahmed, Zachary Garrett, Shanshan Wu, John Rush, and Sushant Prakash. Federated reconstruction: Partially local federated learning. In *Advances in Neural Information Processing Systems (NeurIPS)*, virtual, 2021.
- Martin Slawski and Ping Li. On the trade-off between bit depth and number of samples for a basic approach to structured signal recovery from b-bit quantized linear measurements. *IEEE Trans. Inf. Theory*, 64(6):4159–4178, 2018.
- Adam D. Smith, Shuang Song, and Abhradeep Thakurta. The flajolet-martin sketch itself preserves differential privacy: Private counting with minimal space. In *Advances in Neural Information Processing Systems*, virtual, 2020.
- Jordi Soria-Comas, Josep Domingo-Ferrer, David Sánchez, and David Megías. Individual differential privacy: A utility-preserving formulation of differential privacy guarantees. *IEEE Trans. Inf. Forensics Secur.*, 12(6):1418–1429, 2017.
- Nina Mesing Stausholm. Improved differentially private euclidean distance approximation. In *Proceedings of the 40th ACM SIGMOD-SIGACT-SIGAI Symposium on Principles of Database Systems (PODS)*, pages 42–56, Virtual Event, China, 2021.
- Tyler M. Tomita, James Browne, Cencheng Shen, Jaewon Chung, Jesse Patsolic, Benjamin Falk, Carey E. Priebe, Jason Yim, Randal C. Burns, Mauro Maggioni, and Joshua T. Vogelstein. Sparse projection oblique randomer forests. *J. Mach. Learn. Res.*, 21:104:1–104:39, 2020.
- Santosh S Vempala. *The random projection method*, volume 65. American Mathematical Soc., 2005.
- Stanley L Warner. Randomized response: A survey technique for eliminating evasive answer bias. *Journal of the American Statistical Association*, 60(309):63–69, 1965.
- Kang Wei, Jun Li, Ming Ding, Chuan Ma, Howard H. Yang, Farhad Farokhi, Shi Jin, Tony Q. S. Quek, and H. Vincent Poor. Federated learning with differential privacy: Algorithms and performance analysis. *IEEE Trans. Inf. Forensics Secur.*, 15:3454–3469, 2020.

- Kilian Q. Weinberger, Anirban Dasgupta, John Langford, Alexander J. Smola, and Josh Attenberg. Feature hashing for large scale multitask learning. In *Proceedings of the 26th Annual International Conference on Machine Learning (ICML)*, pages 1113–1120, Montreal, Canada, 2009.
- Jun Wu, Jingrui He, and Jiejun Xu. DEMO-Net: Degree-specific graph neural networks for node and graph classification. In *Proceedings of the 25th ACM SIGKDD International Conference on Knowledge Discovery & Data Mining (KDD)*, pages 406–415, Anchorage, AK, 2019.
- Jia Xu, Zhenjie Zhang, Xiaokui Xiao, Yin Yang, Ge Yu, and Marianne Winslett. Differentially private histogram publication. *VLDB J.*, 22(6):797–822, 2013.
- Zhaozhuo Xu, Beidi Chen, Chaojian Li, Weiyang Liu, Le Song, Yingyan Lin, and Anshumali Shrivastava. Locality sensitive teaching. In *Advances in Neural Information Processing Systems (NeurIPS)*, pages 18049–18062, virtual, 2021.
- Bin Yang, Issei Sato, and Hiroshi Nakagawa. Bayesian differential privacy on correlated data. In *Proceedings of the 2015 ACM SIGMOD International Conference on Management of Data (SIGMOD)*, pages 747–762, Melbourne, Australia, 2015.
- Hang Zhang and Ping Li. Optimal estimator for unlabeled linear regression. In *Proceedings of the 37th International Conference on Machine Learning (ICML)*, pages 11153–11162, Virtual Event, 2020.
- Jun Zhang, Zhenjie Zhang, Xiaokui Xiao, Yin Yang, and Marianne Winslett. Functional mechanism: Regression analysis under differential privacy. *Proc. VLDB Endow.*, 5(11):1364–1375, 2012.
- Jun Zhang, Graham Cormode, Cecilia M. Procopiuc, Divesh Srivastava, and Xiaokui Xiao. Privbayes: private data release via bayesian networks. In *International Conference on Management of Data (SIGMOD)*, pages 1423–1434, Snowbird, UT, 2014.
- Shan Zhang, Lei Wang, Naila Murray, and Piotr Koniusz. Kernelized few-shot object detection with efficient integral aggregation. In *Proceedings of the IEEE/CVF Conference on Computer Vision and Pattern Recognition (CVPR)*, pages 19185–19194, New Orleans, LA, 2022.
- Shijie Zhang, Hongzhi Yin, Tong Chen, Zi Huang, Lizhen Cui, and Xiangliang Zhang. Graph embedding for recommendation against attribute inference attacks. In *Proceedings of the Web Conference (WWW)*, pages 3002–3014, Virtual Event / Ljubljana, Slovenia, 2021.
- Zhaoqi Zhang, Panpan Qi, and Wei Wang. Dynamic malware analysis with feature engineering and feature learning. In *Proceedings of the Thirty-Fourth AAAI Conference on Artificial Intelligence (AAAI)*, pages 1210–1217, New York, NY, 2020.
- Fuheng Zhao, Dan Qiao, Rachel Redberg, Divyakant Agrawal, Amr El Abbadi, and Yu-Xiang Wang. Differentially private linear sketches: Efficient implementations and applications. In *Advances in Neural Information Processing Systems (NeurIPS)*, 2022.
- Argyrios Zymnis, Stephen P. Boyd, and Emmanuel J. Candès. Compressed sensing with quantized measurements. *IEEE Signal Process. Lett.*, 17(2):149–152, 2010.

A Deferred Proofs

A.1 Proof of Lemma 3.6

Lemma 3.6 (Half-normal tail bound). Let X_1, \dots, X_n be iid $N(0, 1)$ random variables and let $Y_i = |X_i|$, $\forall i$. Denote $Z = \sum_{i=1}^n Y_i$. Then for any $t > 0$, it holds that

$$\Pr(Z \geq \sqrt{2n^2 \log 2 + 2nt}) \leq \exp(-t).$$

Proof. By the Markov inequality, we write (with some $\zeta > 0$)

$$\Pr(Z \geq t) = \Pr(\exp(\zeta \sum_{i=1}^n Y_i) \geq \exp(\zeta t)) \leq \frac{\mathbb{E}[\exp(\zeta \sum_{i=1}^n Y_i)]}{\exp(\zeta t)}.$$

By the independence of Y_i and the moment generating function of half-normal distribution, we have

$$\begin{aligned} \mathbb{E}[\exp(\zeta \sum_{i=1}^n Y_i)] &= \prod_{i=1}^n \mathbb{E}[\exp(\zeta Y_i)] = \exp\left(\frac{n\zeta^2}{2}\right) (2\Phi(\zeta))^n = \exp\left(\frac{n\zeta^2}{2} + n \log 2\Phi(\zeta)\right) \\ &\leq \exp\left(\frac{n\zeta^2}{2} + n \log 2\right). \end{aligned}$$

Hence, we have

$$\Pr(Z \geq t) \leq \exp\left(\frac{n\zeta^2}{2} - t\zeta + n \log 2\right),$$

which is minimized at $\zeta = \frac{t}{n}$, leading to

$$\Pr(Z \geq t) \leq \exp\left(-\frac{t^2}{2n} + n \log 2\right).$$

Taking $t = \sqrt{2n^2 \log 2 + 2nt}$ completes the proof. \square

A.2 Proof of Lemma 4.2

Proof. The bivariate normal density function is

$$\begin{aligned} f(x, y) &= \frac{1}{2\pi\sigma_x\sigma_y\sqrt{1-\rho^2}} \exp\left(-\frac{\frac{x^2}{\sigma_x^2} - \frac{2\rho xy}{\sigma_x\sigma_y} + \frac{y^2}{\sigma_y^2}}{2(1-\rho^2)}\right) \\ &= \frac{1}{2\pi\sigma_x\sigma_y\sqrt{1-\rho^2}} \exp\left(-\frac{x^2}{2\sigma_x^2}\right) \exp\left(-\frac{(\frac{y}{\sigma_y} - \rho\frac{x}{\sigma_x})^2}{2(1-\rho^2)}\right). \end{aligned}$$

Therefore, we have $\mathbb{E}[|X| \mid |X| > |Y|] = \frac{A}{P}$, with

$$\begin{aligned} A &= \int_{-\infty}^{\infty} \frac{|x|}{\sqrt{2\pi}\sigma_x\sqrt{1-\rho^2}} \exp\left(-\frac{x^2}{2\sigma_x^2}\right) dx \int_{-|x|}^{|x|} \frac{1}{\sqrt{2\pi}\sigma_y} \exp\left(-\frac{(\frac{y}{\sigma_y} - \rho\frac{x}{\sigma_x})^2}{2(1-\rho^2)}\right) dy, \\ P &= \int_{-\infty}^{\infty} \frac{1}{\sqrt{2\pi}\sigma_x\sqrt{1-\rho^2}} \exp\left(-\frac{x^2}{2\sigma_x^2}\right) dx \int_{-|x|}^{|x|} \frac{1}{\sqrt{2\pi}\sigma_y} \exp\left(-\frac{(\frac{y}{\sigma_y} - \rho\frac{x}{\sigma_x})^2}{2(1-\rho^2)}\right) dy. \end{aligned}$$

Note that $P = Pr(|X| > |Y|)$ in the first statement of the theorem. Our calculation will use the following two identities involving the Gaussian functions (Owen, 1980):

$$\int_0^\infty \phi(ax)\Phi(bx)dx = \frac{1}{2\pi|a|} \left(\frac{\pi}{2} + \tan^{-1} \left(\frac{b}{|a|} \right) \right), \quad (25)$$

$$\int_0^\infty x\phi(ax)\Phi(bx)dx = \frac{1}{2\sqrt{2\pi}} \left(1 + \frac{b}{\sqrt{1+b^2}} \right), \quad (26)$$

where $\phi(x)$ and $\Phi(x)$ are the pdf and cdf of the standard Gaussian distribution.

With a proper change of random variables, we can compute A as

$$\begin{aligned} A &= \int_{-\infty}^\infty \frac{|x|}{\sqrt{2\pi}\sigma_x\sqrt{1-\rho^2}} \exp\left(-\frac{x^2}{2\sigma_x^2}\right) dx \int_{\frac{-|x|}{\sigma_y} - \frac{\rho x}{\sigma_x}}^{\frac{|x|}{\sigma_y} - \frac{\rho x}{\sigma_x}} \frac{\sqrt{1-\rho^2}}{\sqrt{2\pi}} e^{-s^2} ds \\ &= \int_{-\infty}^\infty \frac{|x|}{\sqrt{2\pi}\sigma_x} \exp\left(-\frac{x^2}{2\sigma_x^2}\right) \left[\Phi\left(\frac{|x| - \rho \frac{x}{\sigma_x}}{\sqrt{1-\rho^2}}\right) - \Phi\left(\frac{-|x| - \rho \frac{x}{\sigma_x}}{\sqrt{1-\rho^2}}\right) \right] dx \\ &= \int_{-\infty}^\infty \frac{\sigma_x |t|}{\sqrt{2\pi}} \exp\left(-\frac{t^2}{2}\right) \left[\Phi\left(\frac{\frac{\sigma_x}{\sigma_y} |t| - \rho t}{\sqrt{1-\rho^2}}\right) - \Phi\left(-\frac{\frac{\sigma_x}{\sigma_y} |t| - \rho t}{\sqrt{1-\rho^2}}\right) \right] dt \\ &:= A_1 - A_2. \end{aligned}$$

For the first term we have

$$\begin{aligned} A_1 &= \sigma_x \left[\int_0^\infty \frac{t}{\sqrt{2\pi}} \exp\left(-\frac{t^2}{2}\right) \Phi\left(\frac{\frac{\sigma_x}{\sigma_y} - \rho}{\sqrt{1-\rho^2}} t\right) dt + \int_{-\infty}^0 \frac{-t}{\sqrt{2\pi}} \exp\left(-\frac{t^2}{2}\right) \Phi\left(-\frac{\frac{\sigma_x}{\sigma_y} + \rho}{\sqrt{1-\rho^2}} t\right) dt \right] \\ &= \sigma_x \left[\int_0^\infty \frac{t}{\sqrt{2\pi}} \exp\left(-\frac{t^2}{2}\right) \Phi\left(\frac{\frac{\sigma_x}{\sigma_y} - \rho}{\sqrt{1-\rho^2}} t\right) dt + \int_0^\infty \frac{s}{\sqrt{2\pi}} \exp\left(-\frac{s^2}{2}\right) \Phi\left(\frac{\frac{\sigma_x}{\sigma_y} + \rho}{\sqrt{1-\rho^2}} s\right) ds \right] \\ &= \sigma_x \left[\frac{1}{2\sqrt{2\pi}} \left(1 + \frac{\frac{\frac{\sigma_x}{\sigma_y} - \rho}{\sqrt{1-\rho^2}}}{\sqrt{1 + \frac{(\frac{\sigma_x}{\sigma_y} - \rho)^2}{1-\rho^2}}} \right) + \frac{1}{2\sqrt{2\pi}} \left(1 + \frac{\frac{\frac{\sigma_x}{\sigma_y} + \rho}{\sqrt{1-\rho^2}}}{\sqrt{1 + \frac{(\frac{\sigma_x}{\sigma_y} + \rho)^2}{1-\rho^2}}} \right) \right] \\ &= \sigma_x \left[\frac{1}{\sqrt{2\pi}} + \frac{1}{2\sqrt{2\pi}} \left(\frac{r - \rho}{\sqrt{1 + r^2 - 2r\rho}} + \frac{r + \rho}{\sqrt{1 + r^2 + 2r\rho}} \right) \right], \end{aligned}$$

where we denote $r = \frac{\sigma_x}{\sigma_y}$ and use (26). Similarly, we have that

$$\begin{aligned} A_2 &= \sigma_x \left[\int_0^\infty \frac{t}{\sqrt{2\pi}} \exp\left(-\frac{t^2}{2}\right) \Phi\left(-\frac{r + \rho}{\sqrt{1-\rho^2}} t\right) dt + \int_{-\infty}^0 \frac{-t}{\sqrt{2\pi}} \exp\left(-\frac{t^2}{2}\right) \Phi\left(\frac{r - \rho}{\sqrt{1-\rho^2}} t\right) dt \right] \\ &= \sigma_x \left[\int_0^\infty \frac{t}{\sqrt{2\pi}} \exp\left(-\frac{t^2}{2}\right) \Phi\left(-\frac{r + \rho}{\sqrt{1-\rho^2}} t\right) dt + \int_0^\infty \frac{s}{\sqrt{2\pi}} \exp\left(-\frac{s^2}{2}\right) \Phi\left(-\frac{r - \rho}{\sqrt{1-\rho^2}} s\right) ds \right] \\ &= \sigma_x \left[\frac{1}{\sqrt{2\pi}} - \frac{1}{2\sqrt{2\pi}} \left(\frac{r - \rho}{\sqrt{1 + r^2 - 2r\rho}} + \frac{r + \rho}{\sqrt{1 + r^2 + 2r\rho}} \right) \right]. \end{aligned}$$

Therefore, we obtain

$$A(\rho, r) = A_1 - A_2 = \frac{\sigma_x}{\sqrt{2\pi}} \left(\frac{r - \rho}{\sqrt{1 + r^2 - 2r\rho}} + \frac{r + \rho}{\sqrt{1 + r^2 + 2r\rho}} \right). \quad (27)$$

To compute P , by doing a similar change of variables, we have

$$P = \int_{-\infty}^{\infty} \frac{1}{\sqrt{2\pi}} \exp\left(-\frac{t^2}{2}\right) \left[\Phi\left(\frac{r|t| - \rho t}{\sqrt{1 - \rho^2}}\right) - \Phi\left(-\frac{r|t| - \rho t}{\sqrt{1 - \rho^2}}\right) \right] dt$$

$$:= P_1 - P_2.$$

Using (25), we obtain

$$\begin{aligned} P_1 &= \int_0^{\infty} \frac{1}{\sqrt{2\pi}} \exp\left(-\frac{t^2}{2}\right) \Phi\left(\frac{r - \rho}{\sqrt{1 - \rho^2}} t\right) dt + \int_{-\infty}^0 \frac{1}{\sqrt{2\pi}} \exp\left(-\frac{t^2}{2}\right) \Phi\left(-\frac{r + \rho}{\sqrt{1 - \rho^2}} t\right) dt \\ &= \int_0^{\infty} \frac{1}{\sqrt{2\pi}} \exp\left(-\frac{t^2}{2}\right) \Phi\left(\frac{r - \rho}{\sqrt{1 - \rho^2}} t\right) dt + \int_0^{\infty} \frac{1}{\sqrt{2\pi}} \exp\left(-\frac{s^2}{2}\right) \Phi\left(\frac{r + \rho}{\sqrt{1 - \rho^2}} s\right) ds \\ &= \frac{1}{2\pi} \left(\frac{\pi}{2} + \tan^{-1}\left(\frac{r - \rho}{\sqrt{1 - \rho^2}}\right) \right) + \frac{1}{2\pi} \left(\frac{\pi}{2} + \tan^{-1}\left(\frac{r + \rho}{\sqrt{1 - \rho^2}}\right) \right) \\ &= \frac{1}{2} + \frac{1}{2\pi} \left[\tan^{-1}\left(\frac{r - \rho}{\sqrt{1 - \rho^2}}\right) + \tan^{-1}\left(\frac{r + \rho}{\sqrt{1 - \rho^2}}\right) \right], \\ P_2 &= \frac{1}{2} - \frac{1}{2\pi} \left[\tan^{-1}\left(\frac{r - \rho}{\sqrt{1 - \rho^2}}\right) + \tan^{-1}\left(\frac{r + \rho}{\sqrt{1 - \rho^2}}\right) \right], \end{aligned}$$

which leads to

$$P(\rho, r) = P_1 - P_2 = \frac{1}{\pi} \left[\tan^{-1}\left(\frac{r - \rho}{\sqrt{1 - \rho^2}}\right) + \tan^{-1}\left(\frac{r + \rho}{\sqrt{1 - \rho^2}}\right) \right] \quad (28)$$

Therefore, we know that

$$\mathbb{E}[|X| \mid |X| > |Y|] = \frac{A(\rho, r)}{P(\rho, r)} = \sigma_x \sqrt{\frac{\pi}{2}} \cdot \frac{\frac{r - \rho}{\sqrt{1 + r^2 - 2r\rho}} + \frac{r + \rho}{\sqrt{1 + r^2 + 2r\rho}}}{\tan^{-1}\left(\frac{r - \rho}{\sqrt{1 - \rho^2}}\right) + \tan^{-1}\left(\frac{r + \rho}{\sqrt{1 - \rho^2}}\right)},$$

with $r = \sigma_x / \sigma_y$. We now investigate the derivative of P . By some algebra, we can show that

$$\frac{\partial P(\rho, r)}{\partial \rho} = \frac{2r\rho(r^2 - 1)}{(1 + r^2 - 2r\rho)(1 + r^2 + 2r\rho)\sqrt{1 - \rho^2}}.$$

When $0 < r \leq 1$, $\frac{\partial P(\rho, r)}{\partial \rho} \geq 0$ when $\rho \leq 0$ and $\frac{\partial P(\rho, r)}{\partial \rho} \leq 0$ when $\rho > 0$. Therefore, $\max_{\rho} P(\rho, r) = P(0, r) = \frac{2}{\pi} \tan^{-1}(r)$.

Tail bound. By our previous calculations, the conditional distribution of X given $|X| > |Y|$ is

$$f(x \mid |X| > |Y|) = \frac{\frac{1}{\sqrt{2\pi}} \exp\left(-\frac{x^2}{2}\right) \left[\Phi\left(\frac{r|x| - \rho x}{\sqrt{1 - \rho^2}}\right) - \Phi\left(-\frac{r|x| - \rho x}{\sqrt{1 - \rho^2}}\right) \right]}{P}, \quad x \in \mathbb{R},$$

with $P = Pr(|X| > |Y|)$ in (28) the normalizing constant to make the integral equal to 1.

The conditional tail probability can be computed as follows. For some $t > 0$, by symmetry,

$$\begin{aligned}
& Pr(|X| > t, |X| > |Y|) \\
&= 2 \int_t^\infty \frac{1}{\sqrt{2\pi}\sigma_x} \exp\left(-\frac{x^2}{2\sigma_x^2}\right) \left[\Phi\left(\frac{r|x| - \rho x}{\sqrt{1-\rho^2}}\right) - \Phi\left(-\frac{r|x| - \rho x}{\sqrt{1-\rho^2}}\right) \right] dx \\
&= 2 \int_{\frac{t}{\sigma_x}}^\infty \frac{1}{\sqrt{2\pi}} \exp\left(-\frac{x^2}{2}\right) \left[\Phi\left(\frac{r|x| - \rho x}{\sqrt{1-\rho^2}}\right) - \Phi\left(-\frac{r|x| - \rho x}{\sqrt{1-\rho^2}}\right) \right] dx \\
&:= 2(\tilde{P}_1 - \tilde{P}_2).
\end{aligned}$$

For \tilde{P}_1 , using polar coordinates we have

$$\begin{aligned}
\tilde{P}_1 &= \frac{1}{2\pi} \int_{\frac{t}{\sigma_x}}^\infty e^{-\frac{x^2}{2}} dx \int_{-\infty}^{\frac{r-\rho}{\sqrt{1-\rho^2}}x} e^{-\frac{y^2}{2}} dy \\
&= \frac{1}{2\pi} \int_{-\frac{\pi}{2}}^{\tan^{-1}\left(\frac{r-\rho}{\sqrt{1-\rho^2}}\right)} d\theta \int_{\frac{t}{\sigma_x \cos(\theta)}}^\infty e^{-\frac{r^2}{2}} r dr \\
&= \frac{1}{2\pi} \int_{-\frac{\pi}{2}}^{\tan^{-1}\left(\frac{r-\rho}{\sqrt{1-\rho^2}}\right)} \exp\left(-\frac{t^2}{2\sigma_x^2 \cos^2(\theta)}\right) d\theta.
\end{aligned}$$

Similarly,

$$\tilde{P}_2 = \frac{1}{2\pi} \int_{-\frac{\pi}{2}}^{\tan^{-1}\left(-\frac{r+\rho}{\sqrt{1-\rho^2}}\right)} \exp\left(-\frac{t^2}{2\sigma_x^2 \cos^2(\theta)}\right) d\theta.$$

Therefore, we obtain

$$\begin{aligned}
Pr(|X| > t, |X| > |Y|) &= \frac{1}{\pi} \int_{\tan^{-1}\left(-\frac{r+\rho}{\sqrt{1-\rho^2}}\right)}^{\tan^{-1}\left(\frac{r-\rho}{\sqrt{1-\rho^2}}\right)} \exp\left(-\frac{t^2}{2\sigma_x^2 \cos^2(\theta)}\right) d\theta \\
&= \frac{1}{\pi} \int_{-\tan^{-1}\left(\frac{r+\rho}{\sqrt{1-\rho^2}}\right)}^{\tan^{-1}\left(\frac{r-\rho}{\sqrt{1-\rho^2}}\right)} \exp\left(-\frac{t^2}{2\sigma_x^2 \cos^2(\theta)}\right) d\theta \\
&\leq e^{-\frac{t^2}{2\sigma_x^2}} \frac{1}{\pi} \int_{-\tan^{-1}\left(\frac{r+\rho}{\sqrt{1-\rho^2}}\right)}^{\tan^{-1}\left(\frac{r-\rho}{\sqrt{1-\rho^2}}\right)} d\theta,
\end{aligned}$$

since $\cos^2(\theta) \in [0, 1]$. Notice that P in (28) can be written as $P = \frac{1}{\pi} \int_{-\tan^{-1}\left(\frac{r+\rho}{\sqrt{1-\rho^2}}\right)}^{\tan^{-1}\left(\frac{r-\rho}{\sqrt{1-\rho^2}}\right)} d\theta$. Hence, we know that the conditional tail probability is

$$Pr(|X| > t | |X| > |Y|) = \frac{Pr(|X| > t, |X| > |Y|)}{Pr(|X| > |Y|)} \leq \exp\left(-\frac{t^2}{2\sigma_x^2}\right), \quad \forall r > 0, \rho \in (-1, 1).$$

At the boundaries $\rho = 1$, $\rho = -1$, one can verify $Pr(|X| > |Y|) = 0$. This concludes the proof. \square